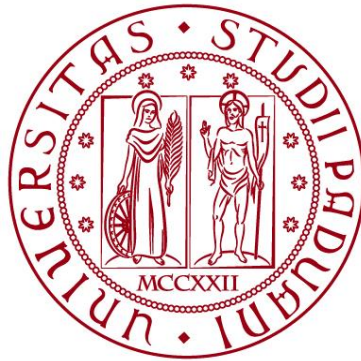


UNIVERSITÀ DEGLI STUDI DI PADOVA
DIPARTIMENTO DI INGEGNERIA CIVILE, EDILE E
AMBIENTALE

Department of Civil, Environmental and Architectural Engineering

Corso di Laurea Magistrale in Environmental Engineering



Master Thesis

**ADSORPTION OF A CRITICAL RAW
MATERIAL (TUNGSTEN) ONTO POROUS
CARBON MATERIALS OBTAINED FROM
RICE WASTES**

Supervisor:
Prof. Eng. Roberto Raga

Laureando: Davide Don
1159898

Host Institution supervisors:
Prof. Eng. Nuno Lapa;
Dr. Maria Bernardo;
MSc Diogo Dias

Academic year 2018-2019

Ringraziamenti

Questa esperienza della tesi in Erasmus è stata intensa sotto molti punti di vista. Passare dal vivere con la propria famiglia, nel piccolo paesino dove si è cresciuti, a vivere per conto proprio nella capitale di uno stato straniero, è qualcosa che porterò con me per sempre.

Mi ha permesso di capire ed apprezzare di più le persone che sono rimaste qui in Italia e di conoscerne di nuove che mi hanno, ognuna a modo loro arricchito. Per questo, sono grato:

Alla mia famiglia, per essere la mia rete di sicurezza mentre provo a spiccare il volo e a trovare il mio posto nel mondo;

Ai miei amici in Italia. La tecnologia non ci ha separati del tutto ma ritrovarvi qui al mio rientro mi ha dato un senso di sicurezza e di fiducia che non so comunicare bene a parole. Grazie di volermi bene sempre e comunque;

Al Professor Raga, per avermi permesso di fare questa esperienza e lavorare su un progetto che mi ha entusiasmato e accresciuto, mentre mi insegnava anche le pene della vita di laboratorio.

To my Erasmus friends, meeting you made me a better person. I am so profoundly grateful for showing me that there are others who think like me and that I could get along with. Thank you for proving me that being as I am is ok. I deeply treasure your friendship.

To Professor Lapa, Maria and the team of the Lab 375. Thank you for welcoming me, supporting me and guiding me during the seven months we spent together. I wouldn't be able to be writing these lines without you.

To my favourite storyteller, the only living person who still knows ancient Italian and my partner in crime/project mate, grazi milli Diogo, por tudo.

Davide

Acknowledgements

This work was partially supported by LAQV-REQUIMTE, which is funded by national funds from FCT/MCTES (UID/QUI/50006/2013) and co-funded by ERDF under the PT2020 Partnership Agreement (POCI-01-0145-FEDER-007265). Davide Don acknowledges the European Commission for the grant attributed through the ERASMUS+ Programme which allowed him to do the internship at FCT-NOVA (Portugal). Davide Don also acknowledges Professor Ana Silveira (DCEA-FCT-NOVA), who is the responsible for the learning agreement between UNL and Padua University, to allow him to develop the internship at FCT-NOVA, and Professor Paulo Sá Caetano (DCT-FCT-NOVA) and the PhD student Mr. André Sanches for making possible the contact with the mining Company that supplied the mining wastewater.

Abstract

The strong industrial development of the last few decades has determined a very high demand for resources, especially materials from metal groups. This led to a high demand for mineral extraction and consequent high flows of metal-contaminated wastewaters.

The high Economic Importance and Supply Risk of Tungsten (W) ensured its inclusion in the European List of Critical Raw Materials. Therefore, the resource recovery from wastes and wastewaters became of primary importance. Although there are well-established conventional treatments for metal removal from liquid effluents, their disadvantages like the incomplete removal, high energy demand and the production of toxic sludges, prompted for the research of more cost-effective technologies.

Adsorption has proved to be a valid technique for treating a broad range of compounds, including heavy metals, and this promoted an increase in the demand of low-cost adsorbents with high metal binding capacities. The porous materials resulting from pyrolysis and gasification, have been studied as possible adsorbents because of their interesting textural and chemical properties. Gasification and pyrolysis convert lignocellulosic materials into an energy-rich gas product (syngas) and into a solid product (char). Among the many feedstocks tested, rice proved to be very appealing due to the very high availability, being staple food for half of the world population, and due to the attracting Low Heating Value (LHV) of its production residues such as husks and straw. To further improve the properties of the chars, they can be physically or chemically activated. The chars used in this work have been chemically activated with Potassium Hydroxide (KOH), Potassium Carbonate (K_2CO_3) and Phosphoric acid (H_3PO_4). The treatment with the first activating agent allowed to achieve a considerable high surface area ($2610 \text{ m}^2\text{g}^{-1}_{AC}$) and volume of the mesopores ($1.14 \text{ cm}^3\text{g}^{-1}_{AC}$), while the second one gave the highest pH_{pzc} value (9.56), and the third activation agent enabled to achieve high silica removal from the solid matrix. This work aimed at investigating (i) the adsorption mechanisms for the Tungstate oxyanion (WO_4^{2-}), (ii) to select and optimize porous carbon materials for achieving the best possible performances with a synthetic solution, (iii) to assess the competition mechanism in a real wastewater, and (iv) to make the adsorbent competitive in comparison to a commercial activated carbon specifically engineered for wastewater treatment.

Char2-KOH was obtained by carbonization in a spherical rotary steel reactor at $475 \text{ }^\circ\text{C}$ for 30 min and subsequently was submitted to impregnation with KOH (weight ratio of 1:4, Char2:KOH),

and activated at 850 °C for 2 h in Argon (Ar) atmosphere, then thoroughly washed with hot distilled water until pH 7-8 and oven-dried to constant weight.

This activated carbon presented the overall best performance in the preliminary assessments with a synthetic solution: 99.92 ± 0.03 % of removal efficiency and an uptake capacity of 44.65 ± 0.62 $\text{mg}_{\text{WO}_4^{2-}}\text{g}^{-1}_{\text{AC}}$ at pH 2 and S/L 1.0 gL^{-1} , while achieving a removal of 55.85 ± 3.91 % and an uptake capacity of 249.45 ± 13.92 $\text{mg}_{\text{WO}_4^{2-}}\text{g}^{-1}_{\text{AC}}$ at pH 2 and S/L 0.1 gL^{-1} . Therefore, these results aided in picking the best carbon among the seven tested and in determining the optimal set of parameters to use in the following steps: a pH of 2 and an S/L of 0.1 g L^{-1} . The following step was the study on the adsorption kinetic of the optimized carbon and of the commercial one (CAC) used for comparison purposes. The tungstate removal for both the ACs were best fitted by a pseudo-second order kinetic model presenting determination coefficients, R^2 , of 0.98 for Char2-KOH and 0.93 for CAC. The former achieved the equilibrium in 1 h, while the latter took 15 h to reach a plateau in the experimental distribution. The study of the adsorption isotherm allowed to achieve the highest value of uptake capacity in the synthetic solution, i.e. 854 ± 48.47 $\text{mg}_{\text{WO}_4^{2-}}\text{g}^{-1}_{\text{AC}}$ while ensuring a high removal efficiency, and this enabled to define the third optimal parameter which was the optimal concentration ($150 \text{ mg}_{\text{WO}_4^{2-}}\text{L}^{-1}$).

The modeling procedure proved that Tungsten generates poly-oxometallates and so the adsorption mechanism is a multi-step one. The best fitting was obtained using a two-step isotherm that enabled to reach a determination coefficient, R^2 , of 0.95.

The conditions used in the study with a synthetic solution have been maintained even during the study on the real wastewater and aided in determining that, in opposition to the expectations, the presence of high amounts of dissolved cations might have promoted the removal process due to salting-out effect. This consideration is being supported by the extremely high values of uptake capacity achieved at the wastewater original pH (pH of 8.11 and q_e of 1123 ± 414.0 $\text{mg}_{\text{WO}_4^{2-}}\text{g}^{-1}_{\text{AC}}$) and at pH 2 (1561 ± 64.57 $\text{mg}_{\text{WO}_4^{2-}}\text{g}^{-1}_{\text{AC}}$). The higher removal efficiency produced at pH 2, 88.99 ± 4.28 % against 58.16 ± 19.07 % at the original pH, confirmed the validity of acid conditions as favorable for this remediation/recovery process.

This work was developed in the framework of Mr. Diogo Dias's PhD thesis. Some data was kindly supplied by Mr. Diogo Dias.

Sommario

Il forte sviluppo industriale degli ultimi decenni ha portato ad una forte richiesta di risorse, specialmente materiali metallici. Questo ha condotto a considerevoli estrazioni minerarie, con conseguenti flussi di acque contaminate da metalli.

La grande importanza economica e il rischio di approvvigionamento del Tungsteno ne hanno assicurato l'inclusione nella lista dei Critical Raw Materials. Pertanto, il recupero di questa risorsa è diventato di primaria importanza, e sebbene vi siano trattamenti convenzionali più affermati per la rimozione dei metalli da effluenti inquinati, i loro svantaggi comprendono la rimozione incompleta, alti consumi energetici e produzione di fanghi tossici. Questo ha indotto quindi, a ricercare strategie di trattamento più efficienti e meno costose.

L'adsorbimento ha dimostrato di essere una tecnica molto valida per trattare una vasta gamma di composti, inclusi i metalli pesanti, e questo ne ha favorito la crescita di una domanda di adsorbenti più economici e che garantiscano alte capacità di catturare metalli. La frazione solida risultante da trattamenti di pirolisi e gassificazione è stata studiata come possibile fonte di adsorbenti, per via delle sue interessanti proprietà chimiche e texturali. La gassificazione e la pirolisi convertono materiali ligno-cellulosici in un fluido altamente energetico (syngas) e in una frazione solida, il char. L'alta disponibilità del riso, essendo elemento base dell'alimentazione di metà della popolazione mondiale, e l'interessante Low Heating Value (LHV) dei suoi scarti di coltivazione (come la paglia e la lolla del riso), l'hanno reso una materia prima molto promettente per la produzione di biochar. Per migliorare ulteriormente le proprietà dei carboni, è possibile attivarli fisicamente o chimicamente. Quelli usati in questo lavoro sono stati attivati chimicamente con Idrossido di Potassio KOH, Carbonato di Potassio K_2CO_3 e Acido Fosforico H_3PO_4 . Il trattamento con il primo agente di attivazione ha permesso di ottenere aree superficiali (fino a $2610 \text{ m}^2\text{g}_{AC}^{-1}$) e volume dei mesopori ($1.14 \text{ cm}^3\text{g}_{AC}^{-1}$) considerevoli, il secondo ha dato il valore di pH_{pzc} più alto (9.56), mentre il terzo agente ha permesso di raggiungere alte rimozioni di silicati dalla matrice solida. (WO_4^{2-}), a selezionare e ottimizzare materiali porosi a base di carbonio per ottenere la miglior performance possibile con una soluzione sintetica, a studiare la competizione in un vero reflu industriale e a rendere il carbone scelto competitivo se confrontato con un carbone attivo commerciale preparato specificamente per il trattamento delle acque.

Char2-KOH è stato il carbone attivo che complessivamente ha dato le performances migliori nella fase preliminare con la soluzione sintetica: $99.92 \pm 0.03 \%$ di efficienza di rimozione ed una capacità di adsorbimento all'equilibrio pari a $44.65 \pm 0.62 \text{ mg}_{WO_4^{2-}}\text{g}_{AC}^{-1}$ a pH 2 e con un S/L di 1.0, mentre ha ottenuto efficienze e capacità di adsorbimento del $55.85 \pm 3.91 \%$ e 249.45 ± 13.92

$\text{mg}_{\text{WO}_4^{2-}}\text{-g}_{\text{AC}}^{-1}$ a pH 2 e con un S/L uguale a 0.1. Di conseguenza questi risultati hanno supportato la scelta del carbone per la fase successiva dello studio tra i sette testati e la scelta dei parametri ottimali da usare negli step successivi: pH of 2 ed S/L di 0.1 g L^{-1} . I passi successivi sono il modello cinetico e delle isoterme di adsorbimento del carbone selezionato de della controparte commerciale (CAC). Entrambi gli ACs sono stati modellati meglio da una cinetica dello pseudo-second'ordine con coefficienti di correlazione, R^2 , of 0.98 per il Char2-KOH e di 0.93 per il CAC. Il primo ha raggiunto la condizione di equilibrio in circa 1 ora mentre per il secondo sono state necessarie 15 ore per raggiungere un plateau nella distribuzione sperimentale. Lo studio delle isoterme di adsorbimento, mantenendo alte efficienze di rimozione, è stato possibile raggiungere anche il valore di capacità di adsorbimento più alto con la soluzione sintetica, pari a $854 \pm 48.47 \text{ mg}_{\text{WO}_4^{2-}}\text{-g}_{\text{AC}}^{-1}$. Questo ha permesso di individuare il terzo parametro ottimale, rappresentato dalla concentrazione ottima di $150 \text{ mg}_{\text{WO}_4^{2-}}\text{L}^{-1}$.

La modellazione ha evidenziato che il Tungsteno genera Polioossometallati, e che quindi il suo adsorbimento è un meccanismo a più step. Il miglior fitting infatti, è stato ottenuto con un modello a due step che ha dato una un coefficiente di correlazione, R^2 , di 0.95.

Le condizioni usate nella soluzione sintetica sono state adottate anche per il refluo reale e hanno permesso di scoprire che, al contrario delle aspettative, la forte presenza di altri ioni disciolti ha favorito la rimozione per via del “salting-out effect”. Questa considerazione è stata dimostrata anche dai valori di capacità di adsorbimento estremamente alti sia al pH normale del refluo (pH uguale a 8.11 e q_e di $1123 \pm 414.0 \text{ mg}_{\text{WO}_4^{2-}}\text{-g}_{\text{AC}}^{-1}$) che a pH 2 ($1561 \pm 64.57 \text{ mg}_{\text{WO}_4^{2-}}\text{-g}_{\text{AC}}^{-1}$). La maggior efficienza di rimozione a pH 2, $88.99 \pm 4.28 \%$ contro $58.16 \pm 19.07 \%$ del pH originale, ha confermato la rilevanza delle condizioni acide per un migliore processo di rimozione/recupero.

Questo lavoro è stato svolto nel contesto del Dottorato del Sig. Diogo Dias. Alcuni dati sono stati gentilmente forniti dal Sig. Diogo Dias.

List of Contents

1. INTRODUCTION.....	1
1.1. RESEARCH OBJECTIVE.....	3
2. LITERATURE REVIEW.....	3
2.1 INTRODUCTION.....	3
2.2 RICE WASTES STREAMS	3
2.3 PYROLYSIS AND GASIFICATION	5
2.4 POROUS CARBON MATERIALS (CHARS AND ACTIVATED CARBONS) IN THE REMOVAL OF METAL IONS FROM AQUEOUS SOLUTIONS	5
2.4.1 Char.....	6
2.4.2 Activated Carbons.....	6
2.4.3 Physical Activation	7
2.4.4 Chemical Activation	7
2.4.5 Adsorption Mechanisms	8
2.5 SIGNIFICANCE OF TUNGSTEN RECOVERY FROM WASTES AND WASTEWATERS.....	10
2.6 PREVIOUS WORKS OF THE TEAM.....	14
3. MATERIALS AND METHODS	16
3.1 POROUS CARBON MATERIALS.....	16
3.1.1 Research strategy #1	16
3.1.2 Research strategy #2	17
3.1.3 Research strategy #3	18
3.1.4 Characterization of the porous carbon materials	18
3.2 REMOVAL ASSAYS OF TUNGSTATE (WO_4^{2-}) FROM AQUEOUS SOLUTION.....	19
3.2.1 Removal assays from a synthetic solution	19
3.2.2 Adsorption assays at different pH values.....	20
3.2.3 Adsorption assays at different S/L ratios	21
3.3 KINETIC STUDY.....	21
3.4 STUDY ON THE ISOTHERMS	21

3.5 ADSORPTION ASSAYS ON A MINING WASTEWATER.....	23
4. RESULTS AND DISCUSSION	25
4.1 CHARACTERIZATION OF THE POROUS CARBON MATERIALS	25
4.2 BATCH ADSORPTION ASSAYS WITH A SYNTHETIC SOLUTION	29
4.3.1 Adsorption assays at different initial pH values	29
4.3.2 Adsorption assays at different S/L ratios	31
4.3 KINETIC MODELLING	33
4.4 ADSORPTION ISOTHERMS	34
4.5 CHARACTERIZATION OF THE MINING WASTEWATER.....	40
4.6 ADSORPTION ASSAYS IN MINING WASTEWATER	42
4.6.1 Batch assays	42
4.6.2. Ions interaction study	44
4.6.3. Ecotoxicological Study	46
5. CONCLUSIONS	47
6. SCIENTIFIC OUTPUT.....	48
REFERENCES.....	49

List of Figures

Figure 1. Adsorption mechanisms of char with metal ions (Adapted from Li et al., 2017)	10
Figure 2. CRM Graph (Deloitte Sustainability et al., 2017)	11
Figure 3. Tungsten Recovery scheme (EC - European Commission, 2014).....	12
Figure 4. EU sourcing averaged 2010-2014 (Adapted from Deloitte Sustainability, 2017).....	13
Figure 5. Tungsten flows in the EU (EC - European Commission, 2014).....	14
Figure 6. WO_4^{2-} removal efficiency (R) (a) and WO_4^{2-} uptake capacity (q_e) (b) of the ACs at different initial pH values. Experimental conditions: Initial WO_4^{2-} concentration = 50 mg L ⁻¹ ; contact time = 24 h; S/L ratio = 1 g L ⁻¹	30
Figure 7. Tungsten speciation with pH (Patrick and Smith, 2000).....	31
Figure 8. WO_4^{2-} removal efficiency (R) (a) and WO_4^{2-} uptake capacity (q_e) (b) of the ACs at different S/L ratios. Experimental conditions: Initial WO_4^{2-} concentration = 50 mg L ⁻¹ ; contact time = 24 h; Initial pH = 2.....	32
Figure 9. Kinetic data of WO_4^{2-} removal for Char2-KOH and CAC adjusted to kinetic models. Experimental conditions: Initial WO_4^{2-} concentration = 50 mg L ⁻¹ ; S/L ratio = 0.1 g L ⁻¹ ; Initial pH = 2. (qt th PF – theoretical uptake capacity calculated with pseudo-first order kinetic model; qt th PS – theoretical uptake capacity calculated with pseudo-second order kinetic model).....	34
Figure 10. WO_4^{2-} removal efficiency (R) (a) and WO_4^{2-} uptake capacity (q_e) (b) of the ACs at different WO_4^{2-} initial concentrations. Experimental conditions: S/L ratio = 0.1 g L ⁻¹ ; contact time = 24 h; Initial pH = 2.....	35
Figure 11. Adsorption isotherm models fitted to experimental data of the activated carbon Char2-KOH. (Lan – Langmuir model; Fr – Freundlich model; Sips – Sips model; RP – Redlich-Peterson model; Step – Step model).	37
Figure 12. Adsorption isotherm models fitted to experimental data of the activated carbon CAC (Lan – Langmuir model; Fr – Freundlich model; Sips – Sips model; RP – Redlich-Peterson model; Step – Step model).	37
Figure 13. Step isotherm model applied on the experimental data of both ACs in order to compare the fitting results.....	38
Figure 14. Removal efficiency (R) (a) and uptake capacity (q_e) (b) of the ACs Char2-KOH and CAC in the two different scenarios tested on the mining wastewater. Experimental conditions: S/L ratio = 0.1 g L ⁻¹ ; contact time = 24 h; Initial pH = 8.11 for the scenario <i>i</i> and pH = 2 for the scenario <i>ii</i>	43

Figure 15. Concentration variation of the Char2-KOH and CAC in $\text{mg}_{\text{WO}_4^{2-}} \text{L}^{-1}$ at pH 8.11 (original pH), scenario i.45

Figure 16. Concentration variation of the Char2-KOH and CAC in $\text{mg}_{\text{WO}_4^{2-}} \text{L}^{-1}$ at (a) pH 8.11, scenario I, and at (b) pH 2, scenario ii.45

List of Tables

Table 1. Textural Properties and pH_{pzc} of the porous carbons.	25
Table 2. Proximate Analysis of the porous carbons (as-received basis)	26
Table 3. Elemental Analysis of the porous carbons (as-received basis)	26
Table 4. Mineral content of the ACs (Mean \pm Std. deviation expressed as $\text{mg kg}^{-1}_{\text{db}}$; $n = 2$; when the value is preceded by “<” it means that the quantification was below detection limit)	27
Table 5. Kinetic parameters obtained with the applied kinetic models.	33
Table 6. Bibliographic comparison on the uptake capacities of different adsorbents for WO_4^{2-} from aqueous media.	36
Table 7. Parameters of isotherm models for Char2-KOH and CAC.....	39
Table 8. pH, conductivity, density and content of solids on the mining wastewater.	40
Table 9. Mineral content of the mining wastewater, before and after decantation (Mean \pm Std. deviation; $n = 2$) and solubility assessment (%).	41
Table 10. Tailing Dam Water Characteristics (adapted from Meng et al., 2018; values in mg L^{-1} , except pH in Sørensen scale)	42
Table 11. Ecotoxicity assessment of the mining wastewater before and after tungstate (WO_4^{2-}) removal assays.....	46

1. INTRODUCTION

The strong industrial development of the last few decades has determined a very high demand for resources, leading to considerable amounts of wastes released in all environmental compartments. Among all the needed materials, many manufacturers rely on the use of metals and/or heavy metals for their activity, leading to a high demand for mineral extraction and consequent high flows of metal-contaminated wastewaters (Fu and Wang, 2011).

The threat posed by metal contamination in water bodies is particularly relevant, due to the general high solubility characterizing these pollutants, and their tendency to be uptaken and bioaccumulated in living organisms (Song and Li, 2015).

Then, it becomes mandatory to establish stringent legal frameworks to regulate the use and disposal of the previously mentioned substances, to develop effective techniques and technologies to treat the waste outputs and to remediate contaminated media.

A metal found in many industrial applications is Tungsten. Its most widely known use was for the filament in incandescence bulbs due to its very high melting point. Tungsten compounds though are employed in various productive processes such as superalloys for blade turbines or steel tools, catalytic agent in chemical reactions, welding alloy for electrodes that do not melt at the temperature of the voltaic arc or plasma contact material (Trasorras et al., 2016).

The high Economic Importance (EI) and Supply Risk (SR) characterizing this resource ensured its inclusion in the European List of Critical Raw Materials (COM(2011)/0025 final). It is noteworthy that this metal has been the entry with the highest EI in all the following updates COM(2014)/297 final and COM(2017)/490 final.

Given these considerations, the resource recovery from waste and wastewaters became of primary importance, and although there are well-established conventional treatments for the metal removal from liquid effluents, such as chemical precipitation, solvent extraction or ion exchange, their disadvantages like the incomplete removal, high energy demand and the production of toxic sludges (Burakov et al., 2018) prompted for the research of more cost-effective technologies.

Adsorption has proved to be a valid technique for treating a broad range of chemical compounds, including heavy metals (Bansal and Goyal, 2005), and this promoted an increase in the demand of low-cost adsorbents with high metal binding capacities.

Over the last years, the chars resulting from pyrolysis and gasification have been studied as possible adsorbent materials (Ahmad et al., 2014) because their textural properties resemble the ones of charcoal or activated carbons, both historically used in the removal of contaminants from liquid and gaseous media.

Gasification and pyrolysis convert biomass materials, particularly lignocellulosic biomass, into liquids and gases with energy and chemical value, and into a solid product, the char. Recently, agricultural wastes have become a promising feed for these thermal processes, because they enable to exploit the "renewable energy" obtained by the fuel and better dispose of the residual fraction. In this way, these thermochemical processes provide both environmental and economic benefits (Ma et al., 2012).

Among the many feedstocks tested, rice proved to be very appealing due to the very high availability and interesting Low Heating Value (LHV) of its production residues, such as the husks and straw (Akgün and Luukkanen, 2012).

Rice is an important staple food for half of the world population (Lim et al., 2012) and a relevant component of the Primary Sector Gross Domestic Product (GDP) in various countries, such as Italy and Portugal.

These two countries could derive particular benefit from further investing in the use of rice waste fractions, or rice wastes blends (rice husks, rice straw and polyethylene from bags used in the transport activities of seeds, for example). In terms of production, Italy is the first producer of rice in EU, while Portugal is the fifth country (FAO, 2018b).

Considering that Portugal provides 17% of the whole EU demand of Tungsten (*SWD(2018) 36 final*) and Italy entirely depends on the import of this metal, this study becomes a very valid exploitation strategy.

This thesis work assumes high relevance from an academic perspective, due to the particularly limited presence of studies on Tungsten removal, and complete absence of previous works on the use of porous carbon materials obtained from rice wastes blends, aside from those already performed by this team.

1.1. RESEARCH OBJECTIVE

The main objective of this Master thesis is to assess the feasibility of using porous carbon materials (chars and activated carbons) from the pyrolysis and gasification of rice waste streams (rice straw, rice husk and polyethylene) in the removal/adsorption of Tungsten (W) from aqueous solutions.

To achieve this main objective, the following specific tasks were defined:

1. Production and optimization of porous carbons materials from rice wastes;
2. Adsorption assays of W under batch conditions, exploiting different experimental conditions;
3. Comparison of the performance of carbon materials with a commercial activated carbon (CAC).

2. LITERATURE REVIEW

2.1 INTRODUCTION

In order to assess the scientific relevance and novelty of the present work, a literature review was performed. This review was focused on the following topics:

1. Wastes produced in rice cultivation and processing (rice waste streams);
2. Characteristics of pyrolysis and gasification processes;
3. Use of porous carbon materials (chars and activated carbons) in the removal of metal ions from aqueous solutions;
4. Tungsten recovery from wastewaters;
5. Previous works from the same research team.

2.2 RICE WASTES STREAMS

Rice (*Oryza sativa*) is the second most produced cereal worldwide (FAO, 2018a). In 2017, the world production was 757 Mt, while in Europe was 4.22 Mt (FAO, 2018b). The most recent statistics identify Italy as the main European producer with a provision of 1.59 Mt, followed by Russia, Spain, Greece, and Portugal as the fifth supplier with 0.169 Mt of paddy rice (FAO, 2018b).

Rice cultivation, collection, and processing generate different waste streams. The most significant ones are Rice Straw (RS), Rice Husk (RH), and the plastic bags (generally made of Polyethylene, PE) used to carry seeds and fertilizers.

Considering the generated biowastes, 1 kg of harvested grain (paddy rice), RH represents about 23% wt of the total paddy rice mass (Prasara-A and Gheewala, 2016), and the same quantity of rice can result in the production of 1.0-1.5 kg of RS (Sangon et al., 2017). This means that even if both by-products could be a burden to properly dispose of, they can represent an interesting resource as well.

In Italy, for example, RS is employed in the manufacture of thermal-insulating panels for bio-construction purposes, and RH is exploited for proteins extraction for feedstock or biofuel production (Bertini et al., 2017), while the PE is mostly recycled or thermally disposed. For comparison in Portugal, RS is either burnt in open-air at the rice fields or directly incorporated in soils, while RH is either used as bed material in poultry farms or as feedstock for animal feeding, and plastics are mechanically treated to be exported and recycled in Asian countries.

Rice bio-wastes can be valorized by resorting to biochemical processes or to thermal ones. The biochemical processes, such as co-composting (Zhou et al., 2015), anaerobic digestion and co-digestion (Iyagba et al., 2009; Jabeen et al., 2015), bio-fermentation for bioethanol production (Binod et al., 2010; Fang et al., 2010), or dark-fermentation for bio-hydrogen production (Zhou et al., 2015), represent some sound possibilities. These technologies require a pre-treatment step to increase the bioavailability of the sugars contained in the polymeric fraction of cellulose and hemicellulose, causing an increasing cost of the final products.

Thermal processes appear to be engaging technologies to valorize these wastes as well. RS, RH and the PE in fact present interesting Lower Heating Values (LHV): 12.4 MJ kg⁻¹ for RS (Delivand et al., 2011), 12.9 MJ kg⁻¹ for RH (Akgün and Luukkanen, 2012), and 44.0 MJ kg⁻¹ for PE (Ahmed et al., 2011).

The possible treatments could then be: direct combustion (Said et al., 2013; Sathitruangsak et al., 2009; Vitali et al., 2013), gasification (Akgün and Luukkanen, 2012; André et al., 2014; Mastellone and Zaccariello, 2013), or pyrolysis (Huang et al., 2015; Pinto et al., 2015).

However, according to the European Waste Framework Directive (Directive 2008/98/EC, 2008), incineration is considered a recovery option only whenever electric energy production is performed, while on the contrary gasification and pyrolysis can also be included in the category of recycling technologies, as organic wastes can be reprocessed into new products for several applications, such as biopolymers, biofuels, syngas and chars.

2.3 PYROLYSIS AND GASIFICATION

Promoting more sensible management and reducing the production of waste has been one of the main concerns in the last couple of decades. Among the various possibilities, thermal treatments represent a valid strategy to transform high carbon-content materials into high-added value intermediate products, such as syngas (in the case of gasification), bio-oils (in the case of pyrolysis), and chars (for both thermal processes). Moreover, by carefully adjusting the operational parameters, both thermal processes can be tailored for promoting the production of one of the products.

Gasification is a thermochemical process that converts carbonaceous resources primarily into a gaseous mixture called syngas (containing CO, H₂, CO₂, CH₄, and smaller quantities of higher hydrocarbons) at temperatures in the range of 600–1500 °C, with an oxygen feed below stoichiometric amount to prevent complete oxidation, and in the presence of a gasifying agent, such as air, steam, oxygen, or carbon dioxide (Motta et al., 2018).

Pyrolysis is the thermochemical decomposition of organic material performed under moderate pressure, at relatively high temperatures (400–800 °C), in the absence of oxygen supply (Arena and Di Gregorio, 2014; Dias et al., 2017; Pinto et al., 1999), while providing an opportunity to transform low-energy density materials into biofuels of high-energy density, at the same time recovering high-value chemicals (Czajczyńska et al., 2017).

Although there are several studies of gasification and pyrolysis using RH (Lim et al., 2012; Ma et al., 2012), RS (Lim et al., 2012; Ma et al., 2012), and PE (Arena and Di Gregorio, 2014; Costa et al., 2007) as fuels, pyrolysis and gasification using blends of these wastes are poorly studied and can be an important topic to explore (Dias et al., 2018a).

2.4 POROUS CARBON MATERIALS (CHARS AND ACTIVATED CARBONS) IN THE REMOVAL OF METAL IONS FROM AQUEOUS SOLUTIONS

Depending on the purpose of the thermal process, syngas and bio-oil production can be favored in comparison to the char, leaving the solid residue as waste to be valorized or be treated.

2.4.1 Char

There are many applications for the char, such as (i) combustion for energy recovery (Henrich et al., 1999), (ii) in-situ catalytic conversion (Shen et al., 2014), (iii) carbon sequestration (Hansen et al., 2014), (iv) soil amendment material (Lehmann et al., 2011), and (v) precursor of activated carbons (Ahmad et al., 2012).

Due to the promising remediation strategies offered by porous carbons materials, there has been increasing interest in using chars (and activated carbons) into water treatment as well (Tan et al., 2015).

Porous carbonaceous materials have been used for a long time as sorbents for organic and inorganic contaminants from liquid and gaseous media. Chars can be listed among those materials and can be considered as precursors of activated carbons, because even if in general they are neither activated nor chemically treated, they present various similarities with activated carbons, although they are less porous (Ahmad et al., 2012; Tan et al., 2015).

Compared with the commercial alternatives, chars are produced from agroforestry by-products or different biowaste fractions, representing a new potentially zero to low-cost substitute in the manufacture of adsorbents. Therefore, this possibility presents significant economic and environmental benefits (Hirunpraditkoon et al., 2011), especially considering a less energy-demanding process.

The specific properties of chars that enable their use as adsorbing agents include relatively high specific surface area, enriched surface functional groups, and presence of mineral components. These qualities are mainly affected by pyrolysis or gasification temperature, residence time, and feedstock type so they must be chosen carefully (Ahmad et al., 2014).

2.4.2 Activated Carbons

The char is a stable carbon-dominant material that becomes an Activated Carbon (AC) by undergoing a physical or chemical activation (or a combination of both) meant to improve its pore structure, surface area and functionality (Kwiatkowski, 2008; Tan et al., 2016). These characteristics are particularly important because a raw char might have a limited ability to selectively adsorb contaminants (Ma et al., 2012), but the activation promotes the presence of enriched surface area and sorption capacity.

The physical activation comprises the reaction between the precursor and an oxidizing gas at high temperatures, while the chemical activation involves the processing of the carbonaceous precursor

with salts, alkali, or acidic compounds, and consequently the carbonization of the degraded input material in an inert atmosphere (Kwiatkowski, 2008).

2.4.3 Physical Activation

The physical activation employs gases or vapors, such as carbon dioxide and steam, to increase the porosity of the char by removing the compounds that can be blocking its pores like the remaining volatile matter after the pyrolysis, and to increase the width of the pores created during the pyrolytic treatment (Kwiatkowski, 2008).

The parameters with the highest importance in physical activation are the time, temperature and activation agent.

The use of carbon dioxide, in fact, favors the formation of microporous structures compared to the use of steam, but the activation is slower because the CO₂ molecule is larger than the water one, hence hindering the diffusion in the char's pores (Kwiatkowski, 2008).

After the physical activation, it is possible to apply chemical oxidative treatments to add oxygenated groups (e.g. carboxyls, lactones, phenols, ketones, quinones, alcohols, and esters) to the activated carbon's surface. This type of treatments generally makes the material more hydrophilic and acidic, lowering its pH_{pzc} and increasing the density of negative charges on the surface.

2.4.4 Chemical Activation

Another type of activation is the chemical activation, which is based on processing the carbon material with salts, alkali, metal hydroxides, carbonates, sulfates, nitrates, as well as nitric, sulfuric and phosphoric acids. Its purpose is to increase the porosity and surface area of the char and to increase the functional groups present on the char's surface (Sizmur et al., 2017).

The first step of the activation process is the impregnation with the solution of the selected activating agent, resulting in the degradation of the input material. The impregnated material undergoes a pyrolytic treatment at a temperature between 400 and 800 °C in an inert atmosphere, generally composed by N₂. This way, it is possible to remove the volatile chemicals occluding the pores and improve the porous area. The third and final step of the activation is the washing of the cooled carbonized product to remove the excess of activation agent.

Alkaline treatments are usually performed using metal hydroxides, such as KOH or NaOH, that increase the hydroxyl functional groups on the char's surface and produce activated carbons with a narrow pore size distribution and well-developed porosity.

On the contrary, acid treatments rely on chemicals such as sulfuric acid, nitric acid or phosphoric acid, which provide more carboxylic groups. Among the acidic activating agents currently used, H₃PO₄ is one of the most tested. This compound provides very high surface areas at relatively low temperatures (400-500 °C), introduces a relatively high amount of stable phosphoric complexes, which contribute to a higher oxidation resistance of the surface (Yahya et al., 2015), and provides more oxygenated functional groups to chemically bind positively charged pollutants (Iriarte-Velasco et al., 2014).

The increased porosity is partially due to pore widening, which suggests that the pore size distribution is closer to the supermicropore and mesopore ranges (Wang and Kaskel, 2012).

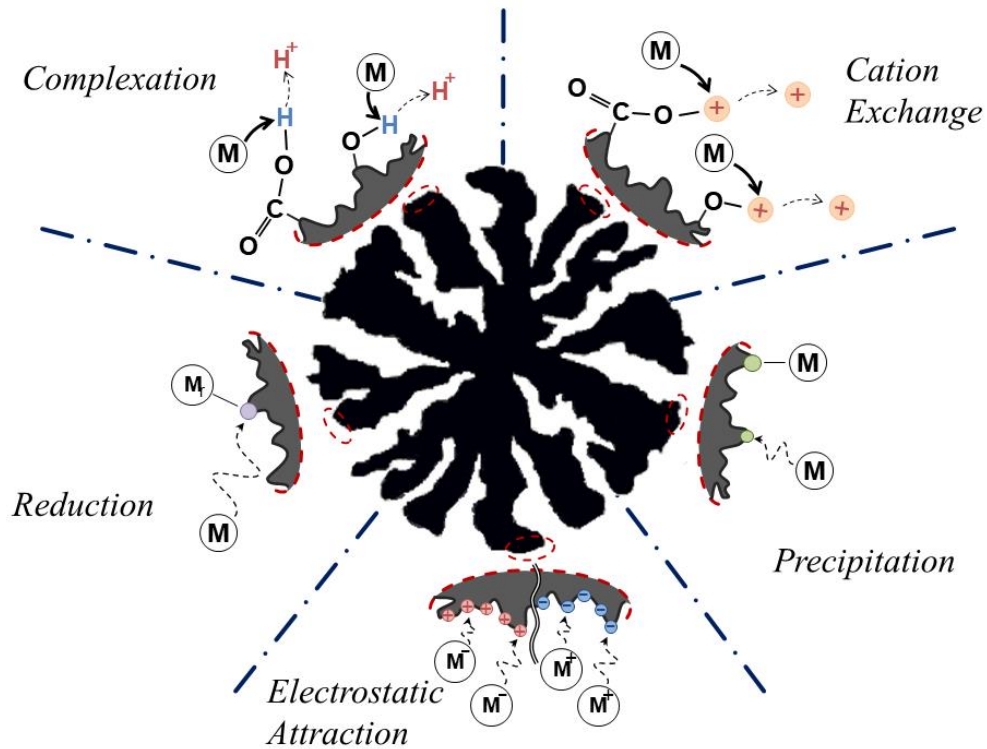
The parameters that mainly affect the properties of the porous structure are the carbonization temperature and the ratio between the mass, or volume, of the activating agent and mass of char. Increasing the temperature enables to achieve higher capacities and larger pore surfaces, but it is influenced by the chosen agent. Generally, the activator on char ratio has the highest influence on the porous structure parameters (Kwiatkowski, 2008).

2.4.5 Adsorption Mechanisms

The high number of pollutants found in aqueous media can be divided into organic and inorganic compounds. The first group is represented mainly by synthetic organic compounds including dyes, pesticides, and pharmaceuticals. The second one is essentially formed by cations and anions (Bansal and Goyal, 2005).

Concerning the inorganic pollutants, the removal using chars or activated carbons can occur by chemical adsorption, precipitation or physical adsorption (less common). Precipitation can be induced by a pH shift in the medium, due to the pH of the char or of the AC (too alkaline or too acid), which determines a change in the metal speciation from a soluble form to an insoluble one, so despite being a removal mechanism, it is not a sorption process. The physical adsorption, often referred as "Pore Filling", happens when the ions are retained in the porous carbon material without involving chemical reactions, while the chemical one implies a strong or weak interaction between the dissolved ions in the diffusive layer around the char, or AC, and the activated sites on the solid. The chemical adsorption of inorganic ions can occur in five different ways:

- (i) Surface precipitation: the carbon surface could have some ions, such as Phosphates (PO_4^{3-}) or Carbonates (CO_3^{2-}), which could then interact with the ones in the aqueous medium and form insoluble compounds that will precipitate on the adsorbent surface;
- (ii) Cation exchange: the adsorbents obtained from gasification or pyrolysis processes may have a high ash content, depending on the biomass feedstock used (Ahmad et al., 2014), and these ashes typically contain Calcium (Ca^{2+}), Potassium (K^+), Sodium (Na^+), and Magnesium (Mg^{2+}) ions (Li *et al.*, 2017). These cations can be replaced by the metal cationic pollutants in the solution releasing the exchanged ones in the medium.
- (iii) Complexation: if the chars or ACs' surface contains atoms with empty electron orbitals, such as oxygen-containing functional groups, the metal ions in the solution will be attracted to the char' surface and complexed with the mentioned functional group.
- (iv) Electrostatic attraction: if the porous material' surface and the metal are both charged with opposing charges, the metal will be attracted to the chars' (or ACs) surface by electrostatic forces.
- (v) Reduction: metallic species can be reduced by gaining electrons from oxygen-surface functional groups, or π - π electrons from the aromatic structures of the adsorbent. Then the reduced metal compound is adsorbed onto the carbon surface.



Legend:

- + Exchangeable metal ions such as Calcium (Ca^{2+}), Potassium (K^+), Sodium (Na^+), and Magnesium (Mg^{2+})
- Ions on the char's/AC's surface such as Phosphates (PO_4^{3-}) or Carbonates (CO_3^{2-})
- + / - Electric charges on the char/AC surface
- M⁺ / M⁻ Metallic Cation or Anion adsorbed
- Electron Donor
- M_r Reduced metal species

Figure 1. Adsorption mechanisms of char with metal ions (Adapted from Li et al., 2017)

2.5 SIGNIFICANCE OF TUNGSTEN RECOVERY FROM WASTES AND WASTEWATERS

Non-energy raw materials are intrinsically linked to industries across all supply chain stages, and so, they are fundamental to any country's economy and to maintain or improve the life quality of its citizens.

This consideration urged the European Commission to launch the “Roadmap to a Resource Efficient Europe” (COM(2011)571 - final) and establish the Critical Raw Material list (CRM List),

with the identification of those with a high supply-risk (SR) and high economic importance (EI) as primary purpose.

Following an objective methodology, this list provides an accurate tool for trade, innovation and industrial policy measures to strengthen the competitiveness of European industries. The list assists in (COM(2017)490 - final):

- identifying the investment needs that could contribute to alleviating Europe's reliance on imports of raw resources;
- guiding and properly support innovations on raw materials supply under the EU's Horizon 2020 research and innovation program;
- drawing attention on the importance of critical raw materials for the transition to a low-carbon, resource-efficient and more circular economy.

The criticality of a raw material is determined by comparing the EI and SR values with established criticality thresholds ($EI > 2.8$ and $SR > 1$), based on the scaled results of the criticality assessments. If a resource reaches or exceeds the threshold values for both parameters is included in the list. Figure 2 shows the CRM list in the form of a graph.

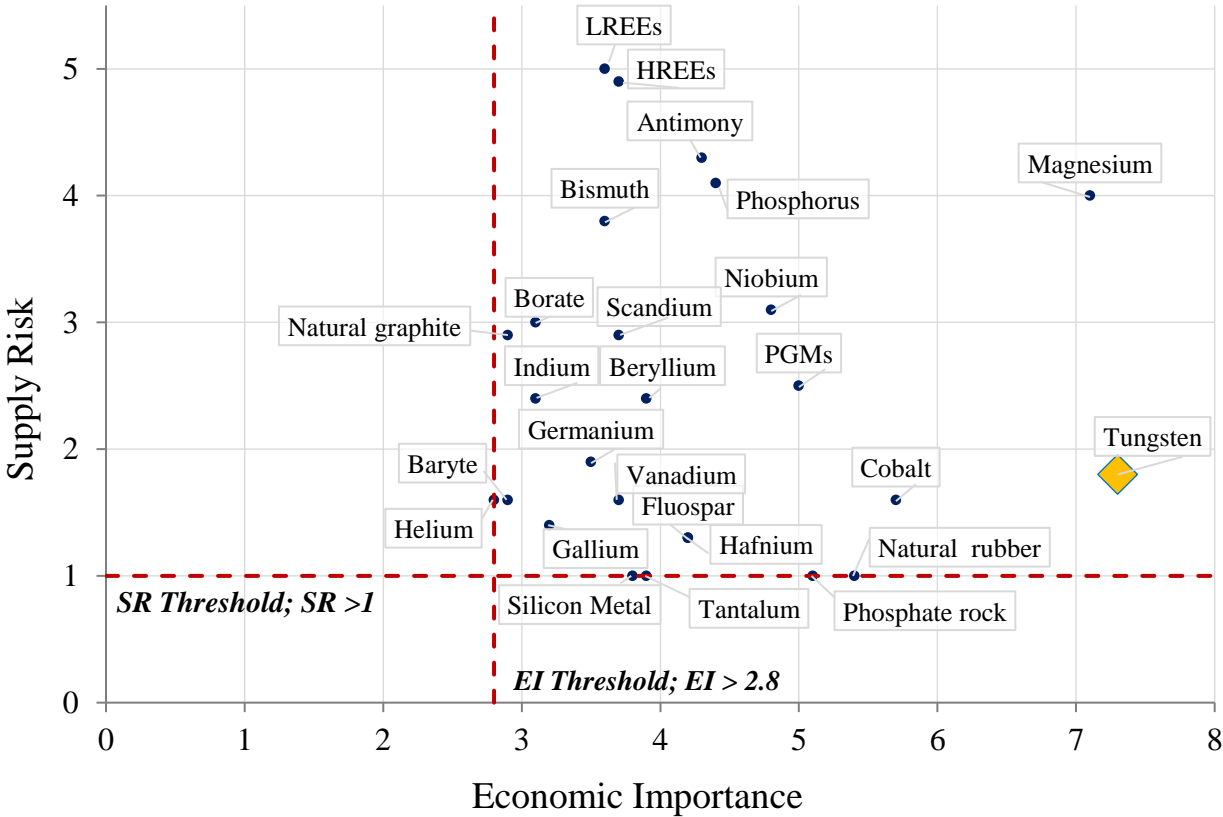


Figure 2. CRM Graph (Deloitte Sustainability et al., 2017)

As shown in Figure 2, the entry with the highest EI is Tungsten (EI = 7.3). It was the material with the highest importance in the first list released in 2011, and in the following updates in 2014 and 2017 as well (Deloitte Sustainability, 2017).

Tungsten (W) is a relatively rare element, it has the highest melting point of all metals, and it has a very high density (19.26 gcm⁻³) (Trasorras et al., 2016). Most of this resource is employed in manufacturing hard steels, whose main component is Tungsten Carbide (WC) due to its remarkable hardness, but the widest range of applications is represented by Tungsten alloys. They include lighting technology, electrical and electronic technology, high-temperature technology (e.g. furnaces, power stations), welding, spark erosion, space travel and aircraft devices, armaments and laser technology, drilling and cutting tools (Deloitte Sustainability, 2017).

The raw material is obtained from mineral extraction and then concentration/upgrading processes. Then, the concentrated ore is mixed with in-process and end-of-life scrap and treated to remove impurities. The most common outcome of these treatments is Ammonium Paratungstate (APT), which it is used to manufacture other tungsten chemicals and products. Figure 3 shows the common W recovery scheme.

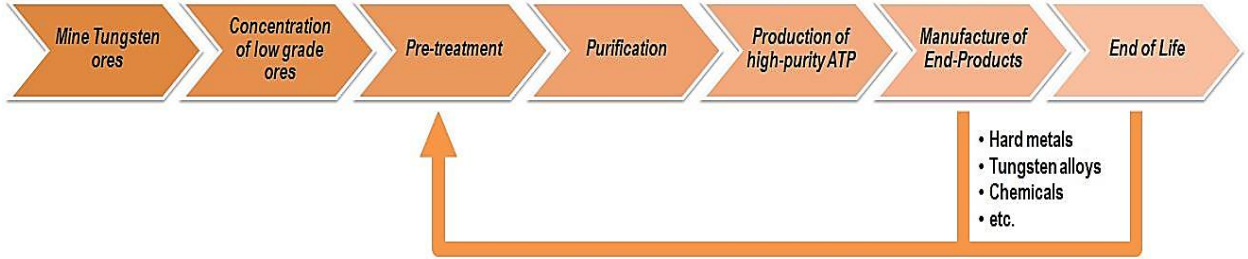


Figure 3. Tungsten Recovery scheme (EC - European Commission, 2014)

Regarding the European economy, the primary source of Tungsten is Russia (50%) followed by Portugal (17%), Spain (15%) and Austria (8%) (Deloitte Sustainability, 2017), as shown in Figure 4.

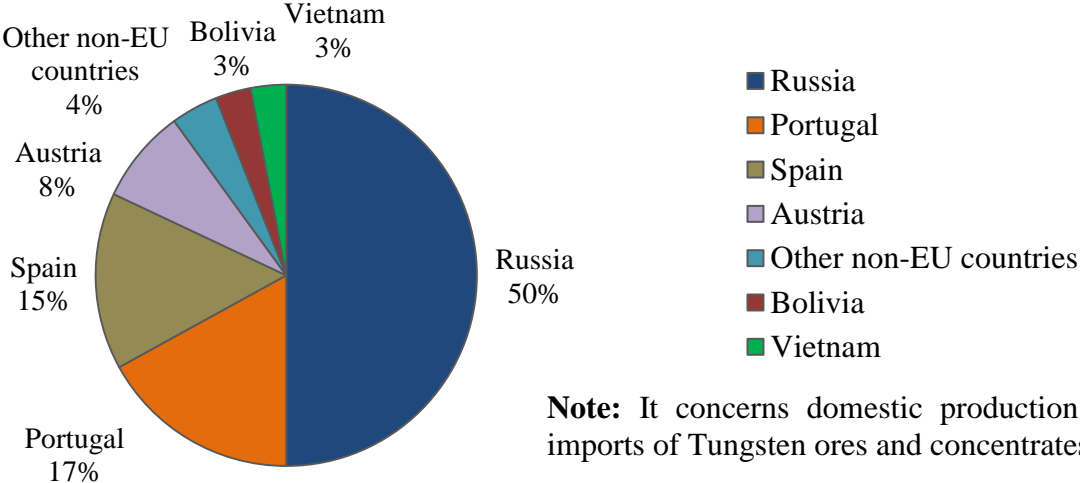


Figure 4. EU sourcing averaged 2010-2014 (Adapted from Deloitte Sustainability, 2017)

The need for recovering and recycling of W is given by its very low substitutability by other metals and its high content in tungsten scraps (up to 90%) compared to tungsten-bearing ores (Trasorras et al., 2016). Its unique properties result in a loss of performance, or an increase in the production costs, when using any substitute that has to be employed to manufacture the same good (EC - European Commission, 2014).

Figure 5 present the Sankey Diagram for the Material Flow Analyses (MFA) of W within the boundaries (dashed line) of EU-28. The arrows represent mass flows (in kg/year) of the chosen material occurring within the system borders, or as import and exports. Their thickness shows the importance of the flow. This type of representation is very efficient in displaying mass balances. The overall sum of inputs must be equal to the outputs. This enables to see that the secondary material flow (purple one), representing the recovered and/or recirculated Tungsten, constitutes 44.9% of the overall W input.

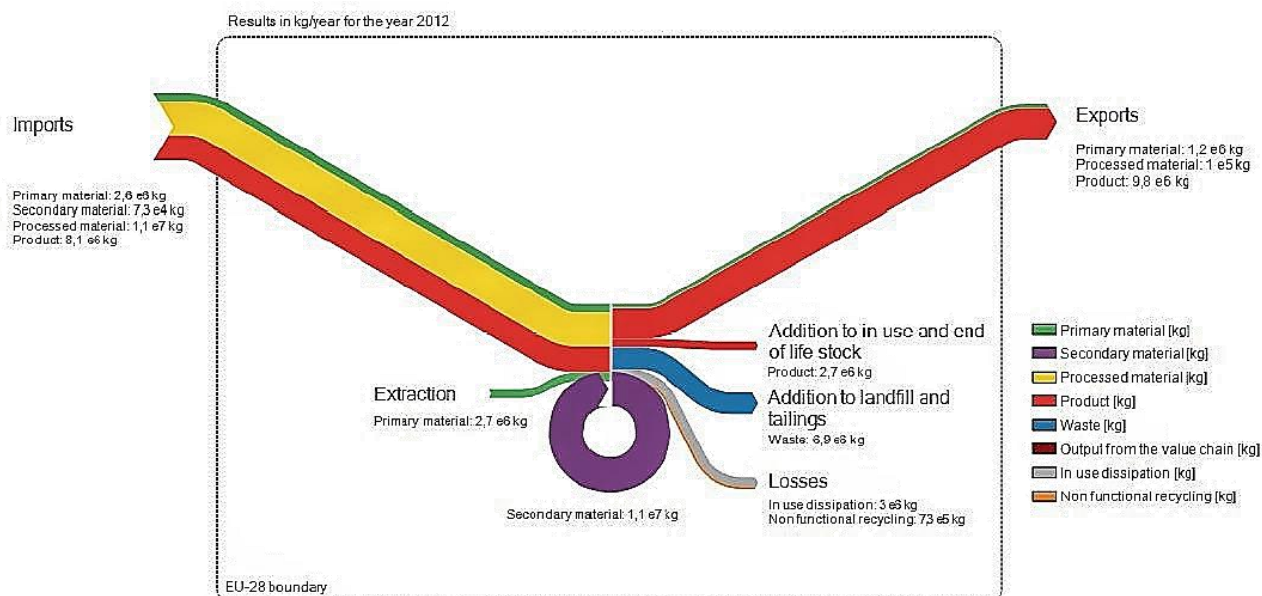


Figure 5. Tungsten flows in the EU (EC - European Commission, 2014)

2.6 PREVIOUS WORKS OF THE TEAM

This Master Thesis is part of a PhD work developed in the Materials for Adsorption and Catalysis (MAC) group of the Faculty of Sciences and Technology (FCT) - NOVA University of Lisbon. This research group belongs to the Research Centre Requimte - Associated Laboratory for Green Chemistry and relied on the support from the team of Dr. Jakpar Jandosov from the Institute of Combustion Problems, Almaty, Kazakhstan, who provided some of the studied activated carbons. Also, a collaboration with the Department of Earth Sciences from FCT-NOVA, namely the Professor Paulo Sá Caetano team was essential to have access to an industrial sludge from a mine in Portugal.

The PhD study in which this Master Thesis was developed is comprised in the framework of the National Project “Ricevalor”, so its primary purpose is to find feasible and effective strategies to add value to rice straw, rice husk and polyethylene resulting as by-products of rice cultivation and processing. The PhD main goals consist in studying the potential valorization of the solid fraction (chars) obtained in the co-pyrolysis and co-gasification of blends of the mentioned rice wastes, as removal agents of Chromium and Tungsten from aqueous solutions.

Tungsten, as mentioned in the previous chapter, is the resource with the highest economic importance in the Critical Raw Material list while Chromium is another entry of the list but also a well-known pollutant and highly relevant for Portuguese and European industries.

The present Master Thesis is going to focus on the Activated Carbons' properties when optimized for W adsorption and all the results are going to be compared with the ones of a commercial activated carbon (CAC) used in a benchmarking practice. This will improve the competitiveness of the adsorbents created in the lab in comparison with an activated carbon already available on the market.

Previous scientific outputs from the team are as follows:

- D. Dias, N. Lapa, M. Bernardo, D. Godinho, I. Fonseca, M. Miranda, F. Pinto and F. Lemos, 2017. Properties of chars from the gasification and pyrolysis of rice waste streams towards their valorisation as adsorbent materials, *Waste Management*, 65, 186–194
- D. Dias, M. Bernardo, N. Lapa, F. Pinto, I. Matos and I. Fonseca, 2018. Activated Carbons from the Co-pyrolysis of Rice Wastes for Cr(III) Removal, *Chemical Engineering Transactions*, vol. 65, 2018, pp. 601-606.
- D. Dias, N. Lapa, M. Bernardo, W. Ribeiro, I. Matos, I. Fonseca and F. Pinto. Cr(III) removal from synthetic and industrial wastewaters by using co-gasification chars of rice waste streams, *Bioresource Technology*, 266 (2018) 139–150.
- J.M. Jandosov, L.I. Mikhalovska, C.A. Howell, D.I. Chenchik, B.K. Kosher, S.B. Lyubchik, J. Silvestre-Albero, N.T. Ablakhanova, G.T. Srailova, S.T. Tuleukhanov, S.V. Mikhalovsky, Synthesis, Morphostructure, Surface Chemistry and Preclinical Studies of Nanoporous Rice Husk-Derived Biochars for Gastrointestinal Detoxification, *Eurasian Chem. J.* 19 (2017) 303.
- J. Jandosov, Z.A. Mansurov, M.A. Bijsenbayev, M.I. Tulepov, Z.R. Ismagilov, N. V. Shikina, I.Z. Ismagilov, I.P. Andrievskaya, Synthesis of Microporous-Mesoporous Carbons from Rice Husk via H₃PO₄-Activation, *Adv. Mater. Res.* 602–604 (2012) 85–89.
- A.R. Satayeva, C.A. Howell, A. V. Korobeinyk, J. Jandosov, V.J. Inglezakis, Z.A. Mansurov, S. V. Mikhalovsky, Investigation of rice husk derived activated carbon for removal of nitrate contamination from water, *Sci. Total Environ.* 630 (2018) 1237–1245.

A short paper on the present work was submitted for oral communication to the international conference “WASTES: Solutions, Treatments and Opportunities 2019” that will be held in Lisboa, between 4 – 6 September 2019 (<https://www.wastes2019.org/>):

After this conference, a full paper will be prepared to be submitted to an international journal indexed in Scopus or WoS.

3. MATERIALS AND METHODS

3.1 POROUS CARBON MATERIALS

The preparation of the porous carbon materials followed three different research strategies:

1) The first strategy involved a first step in which 50 % (w/w) rice husk + 50 % (w/w) polyethylene was submitted to pyrolysis. The char obtained in the pyrolysis process (Char1) was subsequently submitted to different activation treatments which are described below.

2) The second strategy comprised also a first step of pyrolysis of only rice husk and with different experimental conditions from strategy 1. The obtained char (Char2) was also submitted to further activation treatments.

3) The third strategy included the direct carbonization/activation of rice husk with H_3PO_4 .

For comparison purposes, the study was also made on the commercial activated carbon Norit GAC 1240 (CAC).

3.1.1 Research strategy #1

Preparation of Char1

The pyrolysis Char1 was prepared in a 1 L batch reactor Hastelloy C276 (Parr Instruments) (Pinto et al., 1999). After the thermal treatment, the char was separated from the liquid fraction through settling and extraction with n-hexane (hexane/char ratio: 17 mLg⁻¹) in a Soxhlet extractor, during 3 h.

Afterwards, Char1 underwent chemical activation in a cylindrical quartz fixed bed reactor, with three different activating agents: potassium hydroxide (KOH), potassium carbonate (K_2CO_3), and phosphoric acid (H_3PO_4).

Activation of Char1 with KOH

Char1 was submitted to wet impregnation with KOH (Char1-KOH) at a mass ratio of 1:3. The mixture was heated up under stirring at a temperature of 50 °C, for 5 h, then left to cool down and oven dried in order to collect the solid part and proceed with the activation. The activation was performed in a fixed bed quartz reactor placed inside a furnace at a temperature of 800 °C (heating rate of 5 °Cmin⁻¹), for 2 h, in an inert atmosphere of N_2 (steady flow of 150 mLmin⁻¹). After the activation stage, the sample was consecutively washed with hot water until reaching a stable pH

value close to the pH of deionized water (5.5) and subsequently oven-dried. The overall activation yield resulted to be around 40 % (w/w).

Activation of Char1 with K₂CO₃

Char 1 was impregnated, under dry conditions, with K₂CO₃ (Char1-K₂CO₃) at a mass ratio of 1:4 (Char1:K₂CO₃). Then the mixture was placed in the quartz reactor at a temperature of 800 °C (heating rate of 5 °Cmin⁻¹), for 1 h, in an inert atmosphere of N₂ (steady flow of 150 mLmin⁻¹). After the activation stage, the sample was washed as the one treated with KOH. The overall activation yield resulted to be around 44 % (w/w).

Activation of Char1 with H₃PO₄

Char 1 was impregnated with H₃PO₄ (Char1-H₃PO₄) through the wet method by using a mass ratio of 1:3 (Char1:H₃PO₄). The mixture was heated up under stirring at a temperature of 50 °C, for 5 h, then left to cool down and oven-dried in order to collect the solid part and proceed with the activation step. The activation was performed in the same installation described above, at 500 °C (heating rate of 5 °Cmin⁻¹), for 2 h, in an inert N₂ atmosphere (steady flow of 150 mLmin⁻¹). After the activation stage, the sample underwent a post-treatment which consisted in boiling the sample with a solution of 1M NaOH, for 30 min, to promote the removal of silicates and other impurities. After this treatment, the resulting material was consecutively washed with water until stable pH. The overall activation yield resulted to be around 44.7 % (w/w).

3.1.2 Research strategy #2

It should be mentioned that the preparation of Char 2 and the resulting activated carbons were performed by the team of Dr. Jakpar Jandosov from the Institute of Combustion Problems, Kazakhstan and the details were previously published (Jandosov et al., 2012, 2017; Satayeva et al., 2018).

Preparation of Char 2

The rice husk was carbonized in a spherical rotary steel reactor at 475 °C, for 30 min, and the corresponding char (yield around 40 % w/w) was obtained. The char was subsequently boiled in a HCl aqueous solution (1.5 M), for 15 minutes, for demineralization. Then, Char2 was washed three times with distilled water by boiling and decantation. The demineralized Char2 was oven-dried at 105 °C, for 12 hours.

Activation of Char2 with KOH

The demineralized char was submitted to impregnation with KOH (weight ratio of 1:4, Char2:KOH), and activated at 850 °C, for 2 h, in Argon (Ar) atmosphere. Afterwards, it was thoroughly washed with hot distilled water until pH 7-8 and dried to constant weight (yield 18 % w/w). The activated carbon Char2-KOH was then obtained through this procedure.

Activation of Char2 with K₂CO₃

The demineralized char was subsequently mixed with K₂CO₃ at an impregnation weight ratio of 1:4 (Char2:K₂CO₃), for 24 h. Afterwards, it was placed inside a vertical electric furnace and activated at 950 °C, for 1 hour, in Ar atmosphere. The resulting material was washed with 12% KOH solution to remove the residual SiO₂ (desilication), then thoroughly washed with hot distilled water to remove potassium silicate, until pH 7-8. The material was dried overnight, at 105 °C, to originate the activated carbon Char2-K₂CO₃. The total activation efficiency was 32% (w/w).

3.1.3 Research strategy #3

Activation of rice husk with H₃PO₄

The activation of rice husk (RH) with H₃PO₄ followed a weight impregnation ratio of 1:2 (RH:H₃PO₄) and a pre-carbonization step at 200 °C overnight. Then the sample was heated up to a temperature of 500 °C and the temperature was maintained for 1 h. Activation was conducted in self-generated atmosphere. The carbonized material was then washed with hot distiller water to remove the residual phosphoric acid, and subsequently boiled for 30 min with 1 M NaOH solution to remove silica. Then, the sample was thoroughly washed with hot distilled water to remove potassium silicate until pH 7-8 (boiling-sedimentation-decantation). The resulting AC (RH-H₃PO₄) was oven dried for 12 h, at 105 °C. The activation yield was around 30 % (w/w).

3.1.4 Characterization of the porous carbon materials

The chosen carbon materials were submitted to the following characterizations:

- Proximate analysis – it included the moisture content (M) (EN 14774-1), volatile matter (VM) (EN 15148), and ashes (Ash) (EN 14775), at the temperatures defined in ASTM D1762 standard for wood charcoal.

- Elemental analysis – it comprised the determination of CHNS based on ASTM D 5373 and ASTM D4239 standards (LECO CHN 2000 analyzer and Thermo Finnigan-CE Instruments Flash EA 1112 CHNS series analyzer).
- Mineral content – the samples were submitted to microwave-assisted acid digestion with 3 mL H₂O₂ (30 % v/v) + 8 mL HNO₃ (65 % v/v) + 2 mL HF (40 % v/v), followed by a neutralization step with H₃BO₃ (4 % w/v) (EN 15290), followed by quantification of several chemical elements in the acidic eluates by Inductively Coupled Plasma – Atomic Emission Spectroscopy (ICP-AES) (Horiba Jobin-Yvon equipment).
- Textural analysis – it included the quantification of the surface area, pore volume, and pore size distribution through the adsorption-desorption isotherms of N₂, at 77 K, after sample degasification overnight, under vacuum conditions, at 150 °C. The adsorption data were used to calculate the apparent surface area (S_{BET}) through the BET equation. The total pore volume (V_{total}) was determined by the amount of nitrogen adsorbed at the relative pressure P/P₀= 0.99. The micropore volume (V_{micro}) was evaluated by the t-plot method, and the mesopore volume (V_{meso}) was determined by the difference between V_{total} and V_{micro}.
- pH_{pzc} - The pH value at the point of zero charge was performed by preparing ten solutions of 0.1 M NaCl with initial pH values between 2.00 and 12.00. The pH correction was performed with solutions of NaOH and HCl with concentrations between 0.01 to 1 M. 0.1 g of adsorbent was added to 20 mL of each 0.1 M NaCl solution. The mixtures were shaken in a roller-table device, at 150 rpm, for 24 h. pH_{pzc} corresponds to the point where the initial and final pH values are equal.

3.2 REMOVAL ASSAYS OF TUNGSTATE (WO₄²⁻) FROM AQUEOUS SOLUTION

3.2.1 Removal assays from a synthetic solution

The WO₄²⁻ synthetic solution was prepared using a standard Ammonium Tungstate (NH₄)₂WO₄ solution with a concentration of 1000 mg_{WO₄²⁻}L⁻¹ (Scharlau). Solutions with a concentration of 50 ± 5 mg_{WO₄²⁻}L⁻¹ were prepared from this standard solution by appropriate dilution with ultra-pure water (Milli-Q Academic).

The WO₄²⁻ removal assays were performed under batch conditions with the following methodology:

- i. Every assay was prepared by putting a defined amount of carbon material and synthetic solution in a flask, with a specific S/L ratio;
- ii. The flasks were shaken on a roller-table device (INFORS HT Celltron shaker AK 82) with a contact time of 24 h. This promoted the interaction between adsorbate and adsorbent and the diffusion of the pollutant inside the carbon pores. Such time interval ensured reaching the equilibrium between adsorption and desorption processes;
- iii. After the shaking period, the mixtures were filtered using a vacuum pump (Vaccubrand PC 201 NT) over Nitrate cellulose membranes (Whatman[®] ME 25/21 ST, 47 mm) with a porosity of 0.45 μm .
- iv. The final pH was measured and then the samples were acidified with HCl (37 % v/v) to $\text{pH} < 2.0$ for WO_4^{2-} quantification through ICP-AES.

The removal efficiency, R (%), and adsorbent uptake capacity, q_e ($\text{mg}_{\text{WO}_4^{2-}}\text{g}_{\text{AC}}^{-1}$), were calculated by using equations 1 and 2, respectively:

$$R (\%) = \frac{(c_0 - c_f)}{c_0} \times 100 \quad (1)$$

$$q_e = \frac{(c_0 - c_f)}{m} \times V \quad (2)$$

where C_0 and C_f are the WO_4^{2-} concentrations ($\text{mg}_{\text{WO}_4^{2-}}\text{L}^{-1}$) before and after the adsorption batch assays, respectively, m is the mass of the carbon adsorbent (g) and V is the volume of WO_4^{2-} solution (L).

3.2.2 Adsorption assays at different pH values

This set of assays was meant to study how the adsorption is affected by the pH of the medium. Since Tungstate is a Poly-oxometallate (POM), its speciation and characteristics change with the pH. The pH values tested in the present study were between 2 and 10. The samples were prepared with 20 mg of carbon and 20 mL of solution, ensuring a Solid to Liquid (S/L) ratio of 1 g L^{-1} .

The adsorption procedure (shaking, filtration and characterizations) followed the same steps referred in the section 3.2.1.

3.2.3 Adsorption assays at different S/L ratios

The second set of adsorption assays focused on determining the best S/L ratio for the adsorption process. After comparing the results obtained for the series of activated carbons produced from Char1 and Char2 and CAC, it was possible to define which was the best pH for the next step of the research work. Fixing the pH of the solution at 2 and the mass of carbon at 20 mg_{AC}, the volume was changed to have S/L ratios of 0.1, 0.25 and 1 g L⁻¹ (200 mL, 80 mL and 20 mL of synthetic solution, respectively).

This test allowed to define the best S/L ratio to be used in the kinetic study.

3.3 KINETIC STUDY

The carbons that performed better in the previous studies (Char2-KOH and CAC) were submitted to a kinetic study. The initial conditions were as follows:

- (a) WO₄²⁻ initial concentration: 50 mg_{WO₄²⁻}L⁻¹;
- (b) Initial pH: 2;
- (c) S/L ratio: 0.10 g L⁻¹, which was the S/L ratio that performed better in the preliminary studies.
- (d) Contact times: they ranged between 0.083 h (5 min) and 48 h.

The results have been adjusted using the Non-Linear Least Square method to the Lagergren's pseudo-first order non-linear kinetic model by equation (3) (Lagergren, 1898; Sharma et al., 1990) and to the pseudo-second order non-linear kinetic model by equation (4) (Ho and McKay, 1998):

$$q_t = q_e \times [1 - e^{-k_f t}] \quad (3)$$

$$q_t = \frac{k_s \times q_e^2 \times t}{1 + q_e \times k_s \times t} \quad (4)$$

where q_t is the adsorbent uptake capacity at time t (mg g⁻¹), q_e is the adsorbent uptake capacity in the equilibrium (mg g⁻¹), k_f is the pseudo-first order constant (min⁻¹), k_s is the pseudo-second order constant (g mg⁻¹ min⁻¹) and t is the contact time (min).

3.4 STUDY ON THE ISOTHERMS

Maintaining the purpose of optimizing the selected carbon to be comparable or performing better than the commercial one, the adsorption study was performed on the ACs Char2-KOH and CAC.

The assays were performed with a contact time of 24 h to ensure that the equilibrium conditions were reached, at pH 2 and with a S/L ratio of 0.10 g L⁻¹, which was the optimum ratio identified in the previous adsorption assays.

The concentrations were: 10, 30, 50, 75, 100, 150 and 200 mg_{WO₄²⁻} L⁻¹.

Consequently, the experimental values of uptake capacity q_e have been modeled using five different models:

- the widely used Langmuir and Freundlich isotherms described by equations (5) and (6) (Freundlich, 1907; Langmuir, 1918);
- the Sips model and Redlich-Peterson model described by equations (7) and (8) (Pérez-Marín et al., 2007; Redlich and Peterson, 1958; Sips, 1948);
- the step Isotherm model expressed by the Czinkota equation (9) (Czinkota et al., 2002).

Langmuir's Isotherm

$$q_e = \frac{q_{max}bC_e}{1 + bC_e} \quad (5)$$

where C_e (mg L⁻¹) and q_e (mg g⁻¹_{AC}) are the equilibrium concentrations in the liquid and solid phase, respectively. q_{max} is a Langmuir constant that expresses the maximum adsorbate uptake capacity (mg g⁻¹_{AC}) and b is also a Langmuir constant related to the energy of adsorption and affinity of the sorbent.

Freundlich's isotherm

Freundlich expression is an exponential equation and therefore assumes that the concentration of adsorbate on the adsorbent surface increases with the adsorbate concentration.

$$q_e = k_F C_e^{1/n} \quad (6)$$

where K_F (mg¹⁻ⁿ (L)ⁿg⁻¹) and n are Freundlich's constants, indicating the adsorption capacity and adsorption intensity, respectively.

Sip's Isotherm

The Sip's isotherm is a combination of the Langmuir and Freundlich models and is written as indicated in equation (7):

$$q_e = \frac{q_{max} b C_e^{1/n}}{1 + b C_e^{1/n}} \quad (7)$$

At low sorbate concentrations, it reduces to a Freundlich's isotherm, while at high sorbate concentrations it predicts a monolayer adsorption characteristic of the Langmuir's isotherm.

Redlich–Petersons' isotherm

$$q_e = \frac{k_{RP} C_e}{1 + a_{RP} C_e^\beta} \quad \text{where } \beta \leq 1 \quad (8)$$

This model is similar to the Sip's one but with some differences in the exponent of the experimental concentration at the numerator and in the definition of the coefficients. In fact, K_{RP} ($L g^{-1}$), a_{RP} ($L mg^{-1}$) and β are Redlich–Peterson isotherm constants. This equation reduces to a linear isotherm in the case of low surface coverage and to a Langmuir isotherm when $\beta = 1$.

Step isotherm

The step isotherm is based on the observation that complex cases, where more than one mechanism plays a role in the overall adsorption, can be modeled by a sum of separated contributions.

Starting from the theory of adsorption (Czinkota et al., 2002), it's possible to derive the following equation (Tolner, 2008):

$$q_e = \sum_{i=1}^s \left\{ \frac{a_i k_i [(c-b_i) + a b s (c-b_i)]^{n_i}}{2^{n_i} + k_i [(c-b_i) + a b s (c-b_i)]^{n_i}} \right\} \quad (9)$$

where s is the total number of steps, n indicates the average degree of association of the solute, C is the pollutant concentration ($mg L^{-1}$), K is the adsorption equilibrium constant ($L mg^{-1}$) ^{n} and a is the maximum uptake capacity ($mg g^{-1}_{AC}$) of the layer n_i . The parameter b describes the limit concentration ($mg L^{-1}$) at which the process in the previous step is considered complete and the following one begins.

3.5 ADSORPTION ASSAYS ON A MINING WASTEWATER

Part of this work consisted also in testing the behavior of the selected carbons in a real wastewater coming from a Wolframite mine.

3.5.1 Physical-chemical characterization

The industrial wastewater was characterized for:

- pH (glass electrode with temperature compensation of Hanna Instruments);
- Conductivity (conductivity cell of Thermo, ORION);
- Total Solids (TS) after evaporation and drying at 105 °C;
- Fixed Solids (FS) after calcination at 550 °C;
- Volatile Solids (VS) as the difference between TS and FS;
- Suspended Solids (SS) after filtration through cellulose nitrate membranes (Whatman® ME 25/21 ST, 47 mm) with a porosity of 0.45 µm;
- Total mineral content. The wastewater as a whole was submitted to a microwave-assisted acid digestion with 3 mL HCl (37 % v/v) + 9 mL HNO₃ (65 % v/v) (USEPA 3051A), and the resulting acidic eluate was quantified for several chemical elements by ICP-AES;
- Mineral content of the Filtrate. The wastewater was left to decantation and the upper liquid was filtrated through cellulose nitrate membranes (Whatman® ME 25/21 ST, 47 mm) with a porosity of 0.45 µm and the filtrates were quantified for several chemical elements by ICP-AES.
- Solubility of the species in the wastewater. It has been obtained by a ratio between the elemental concentration in the decanted wastewater (the Filtrate) and in the acidic eluate (equation 10).

$$Solubility (\%) = \frac{[X]_{Filtrate}}{[X]_{Acidic\ eluate}} \times 100 \quad (10)$$

- Ecotoxicity assessment by using the Microtox® assay (ISO 11348-3). In this ecotoxicity assay, the bioluminescence inhibition of the bacterium *Vibrio fischeri* is evaluated after 30 min of exposure to the sample. The result is expressed as the effective concentration of the sample that promotes 50% decrease on the *V. fischeri* bioluminescence (EC_{50-30 min}, % v/v). The lower is the EC₅₀ value, the highest is the ecotoxicity level of the sample for the bacterium.

3.5.2 Adsorption assays

The adsorption assays on the real effluent followed the same procedure as for the synthetic solution described in section 3.2.3 (S/L ratio of 0.1 g L⁻¹ and a contact time of 24 h). This set of assays tested two different scenarios aimed at comparing the performance of the selected carbon, under optimal conditions of pH 2 and under the conditions of the wastewater as supplied by the mining Company. It should be mentioned that these adsorption assays were performed with the filtrated

liquid resulting from the decantation process of the real wastewater, but it will be referred as simply wastewater.

The two scenarios were as follows:

- i. Wastewater with spiked Tungsten at the original pH;
- ii. Wastewater with spiked Tungsten at pH 2.

The mining wastewater was spiked with Tungsten to match the value that gave the highest uptake capacity for the AC named as Char2-KOH in the isotherm modeling assays.

This set of assays enables to study (i) the competition mechanism with other anions, (ii) the salting-out effect due to the presence of cationic species reducing the available solvent due to ionic hydration, and (iii) the release by ACs of other compounds to the medium. This last aspect becomes particularly relevant in remediation techniques, in which it is necessary to understand whether the carbon would remove a pollutant while at the same time releasing other toxic or hazardous substances.

Therefore, a study on the behavior of other species in the medium before and after the adsorption assays was performed, as well as an ecotoxicological evaluation using the Microtox® assay.

4. RESULTS AND DISCUSSION

4.1 CHARACTERIZATION OF THE POROUS CARBON MATERIALS

Tables 1, 2 and 3 present the textural properties, pH_{pzc} , proximate and elemental analysis of the produced porous carbons.

Table 1. Textural Properties and pH_{pzc} of the porous carbons.

Activated carbon	Impregnation Ratio	S_{BET} ($\text{m}^2 \text{g}^{-1}$)	V_{micro} ($\text{cm}^3 \text{g}^{-1}$)	V_{meso} ($\text{cm}^3 \text{g}^{-1}$)	V_{total} ($\text{cm}^3 \text{g}^{-1}$)	pH_{pzc}
Char1-KOH	1:3	1315	0.47	0.13	0.60	4.00
Char1-K ₂ CO ₃	1:4	790	0.26	0.18	0.44	3.93
Char1-H ₃ PO ₄	1:3	554	0.19	0.09	0.28	2.38
Char2-KOH	1:4	2610	0.60	1.14	1.74	6.92
Char2-K ₂ CO ₃	1:4	1151	0.28	0.63	0.91	9.56
RH-H ₃ PO ₄	1:2	1402	0.29	1.11	1.40	6.14
CAC*	na	1030	0.30	0.26	0.56	9.10

na: not applicable; *CAC characterization is taken from (Dias et al., 2018b)

Char2-KOH was the carbon with the highest surface area ($2610 \text{ m}^2 \text{ g}^{-1}$), while Char1-H₃PO₄ was the one with the lowest ($554 \text{ m}^2 \text{ g}^{-1}$). The chars activated with KOH were the ones with the highest micropore volume. It should be noted that the activated carbons obtained from Char2 presented higher mesopore volumes compared to the micropore volumes, while the activated carbons produced from the Char1 presented higher micropore volumes compared to the mesopore volumes. Char1-H₃PO₄ and RH-H₃PO₄ were the two with the lowest pH_{pzc} in their respective groups, as it can be expected considering that H₃PO₄ enables to incorporate strong acidic functionalities at carbons surface. On the other hand, Char2-K₂CO₃ and CAC presented the highest pH_{pzc} values. Overall, the activated carbons from the Char2 and RH series presented higher pH_{pzc} values.

Table 2. Proximate Analysis of the porous carbons (as-received basis)

Activated carbon	Moisture Content (MC) [% w/w]	Volatile matter (VM) [% w/w]	Ashes [% w/w]	Fixed Carbon (FC)* [% w/w]
Char1-KOH	4.52	29.8	1.58	64.1
Char1-K ₂ CO ₃	5.67	37.2	4.53	52.6
Char1-H ₃ PO ₄	12.1	25.0	9.30	53.6
Char2-KOH	8.28	40.6	2.12	49.0
Char2-K ₂ CO ₃	5.62	35.9	6.58	51.9
RH-H ₃ PO ₄	10.8	23.7	3.40	62.1
CAC**	13.1	7.02	5.68	74.2

*FC = 100 – (MC + VM + Ashes); **CAC characterization is taken from Dias et al. (2018b)

Char1-H₃PO₄ and RH-H₃PO₄ were the two ACs with the highest moisture content, indicating that these carbons are quite hydrophilic. All samples presented low ash contents, although samples Char1-H₃PO₄ and Char2-K₂CO₃ presented values between 6.58 – 9.30 % w/w.

Table 3. Elemental Analysis of the porous carbons (as-received basis)

Activated carbon	C [% w/w]	H [% w/w]	N [% w/w]	S [% w/w]
Char1-KOH	83.5	0.33	0.85	<0.03
Char1-K ₂ CO ₃	78.6	0.48	0.80	<0.03
Char1-H ₃ PO ₄	67.9	2.12	0.77	<0.03
Char2-KOH	83.8	0.06	0.57	<0.03
Char2-K ₂ CO ₃	84.0	0.04	<0.20	<0.03
RH-H ₃ PO ₄	79.7	0.55	0.43	<0.03
CAC*	86.3	0.47	<0.20	0.57

*CAC characterization is taken from Dias et al. (2018b)

As shown in Table 3 all the adsorbents presented a high carbon content which indicates a successful conversion of the volatile matter into fixed carbon.

Table 4. Mineral content of the ACs (Mean \pm Std. deviation expressed as mg kg⁻¹_{db}; n = 2; when the value is preceded by “<” it means that the quantification was below detection limit)

Element	Char1-KOH	Char1-K ₂ CO ₃	Char1-H ₃ PO ₄	Char2-KOH	Char2- K ₂ CO ₃	RH- H ₃ PO ₄	CAC*
Si	10030 \pm 822	23076 \pm 1425	3890 \pm 273	920 \pm 91	6470 \pm 127	431 \pm 36	14629 \pm 681
Ca	1833 \pm 117	3605 \pm 311	3877 \pm 373	2310 \pm 92	4577 \pm 416	154 \pm 10	1642 \pm 41
Na	736 \pm 65	413 \pm 33	2013 \pm 99	< 4.36 x10 ⁻²	< 4.24 x10 ⁻²	200 \pm 5	53.4 \pm 0.7
Mg	390 \pm 27	1147 \pm 112	856 \pm 62	848 \pm 14	2230 \pm 53	101 \pm 1	444 \pm 20
Fe	682 \pm 6	511 \pm 45	212 \pm 18	6873 \pm 171	7810 \pm 627	149.79 \pm 4.67	3182 \pm 228
Al	578 \pm 26	638 \pm 45	91.5 \pm 6.8	17.3 \pm 1.0	138 \pm 1	< 1.12	8780 \pm 23
K	188 \pm 12	390 \pm 20	232 \pm 7	2499 \pm 35	24960 \pm 967	58.0 \pm 4.3	1032 \pm 3
Zn	292 \pm 17	97.8 \pm 2.6	124 \pm 10	20.3 \pm 0.7	16.6 \pm 0.2	16.9 \pm 0.3	3.91 \pm 0.06
Ti	79.6 \pm 4.9	80.8 \pm 15.1	52.4 \pm 1.1	< 1.09	< 1.06	< 1.12	626 \pm 14
Ba	24.0 \pm 1.5	35.8 \pm 3.5	69.6 \pm 5.6	11.9 \pm 1.0	16.9 \pm 1.4	4.32 \pm 0.39	112 \pm 6
Cr	51.7 \pm 4.4	40.4 \pm 3.9	20.3 \pm 1.4	293 \pm 14	217 \pm 5	< 0.381	265 \pm 16
Ni	42.6 \pm 1.8	25.0 \pm 1.2	< 3.03	82.8 \pm 2.5	< 0.848	< 0.897	22.6 \pm 1.0
Cu	15.2 \pm 0.1	20.5 \pm 1.0	15.3 \pm 1.1	12.8 \pm 0.1	46.5 \pm 3.4	< 0.852	26.7 \pm 2.1
W	< 6.98	< 7.08	< 7.58	< 2.18	< 2.12	< 2.24	< 2.21
Se	< 3.49	< 3.54	< 3.79	< 1.09	< 1.06	< 1.12	< 1.51
Mo	< 0.419	< 0.425	< 0.455	< 0.131_	< 0.127	< 0.135	< 0.138
Pb	< 0.349	< 0.354	< 0.379	< 0.109_	< 0.106	< 0.112	< 0.115
Sb	< 0.349	< 0.354	< 0.379	< 0.109	< 0.106	< 0.112	9.21 \pm 0.38
As	< 0.349	< 0.354	< 0.379	< 0.109	< 0.106	< 0.112	6.68 \pm 0.54
Cd	< 0.279	< 0.283	< 0.303_	< 8.72 x10 ⁻²	< 8.48x10 ⁻²	< 8.97 x10 ⁻² _	< 9.21 x10 ⁻²
Hg	< 2.09 x10 ⁻²	< 2.13 x10 ⁻²	< 2.27 x10 ⁻²	< 6.54 x10 ⁻³	< 6.36 x10 ⁻³	< 6.73 x10 ⁻³	< 6.91 x10 ⁻³

* CAC characterization is taken from (Dias et al., 2018b)

All the ACs containing RH presented high silicon content (aside from the RH-H₃PO₄ which was washed with NaOH to specifically remove silicates), due to the presence of this chemical element in the composition of pristine biomasses (Dias et al., 2017; Jandosov et al., 2012, 2017). It is interesting to note that even the CAC presented a high Si content, meaning that the raw material used for its manufacture was rich in that element. The different origin of the biomass-based ACs compared to the commercial one can be noted by comparing the values of Cr, Ti, Sb and As, which were much higher in CAC. It is interesting to note that due to the presence of PE in the composition of the Char1 group the value of Ti is significantly higher compared to Char2 (while still being considerably lower than CAC). This can be explained considering that Ti was a pigment added to the plastic bags to give them the desired color and, while the PE and other volatile matters were converted to bio-oil during the pyrolysis of the feedstock, Titanium remained in the solid fraction and became part of the char. There aren't signs that suggest that this difference affected the removal capacity of the ACs. The carbons activated with K₂CO₃ retained the highest concentration of K. Overall, all the ACs were rich in alkaline and alkaline-earth elements such as Ca, Na, Mg, K, but also Fe and Al were present with significative amounts.

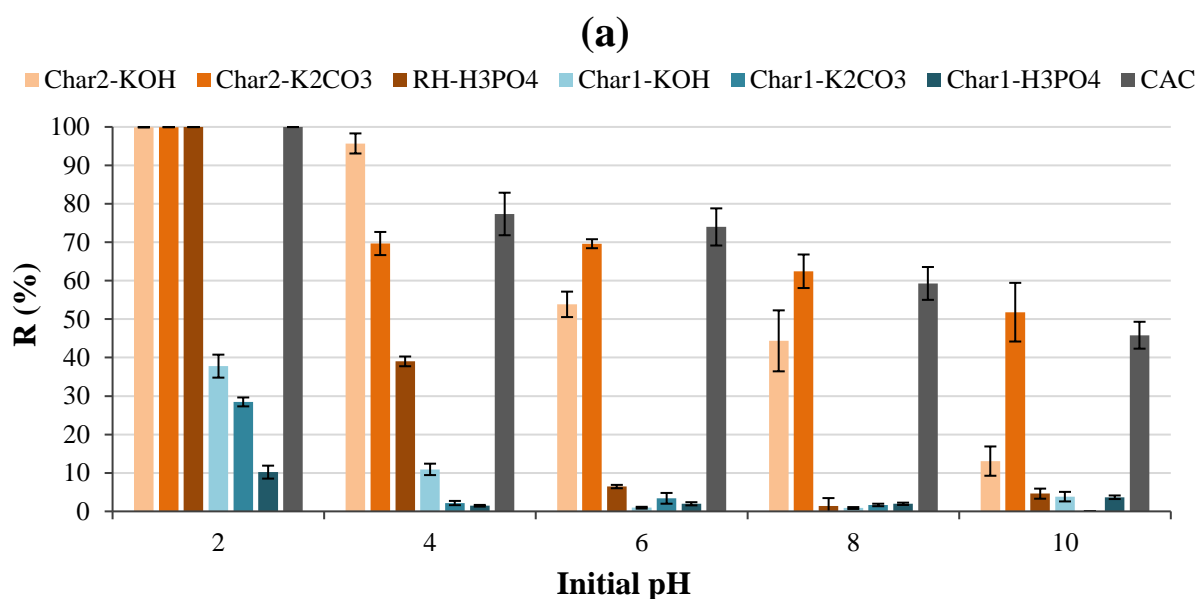
4.2 BATCH ADSORPTION ASSAYS WITH A SYNTHETIC SOLUTION

Some of the aims of this research work were (i) to optimize chars into porous carbons for the adsorption of Tungstate (WO_4^{2-}) and (ii) to identify which of them gave the best overall performance as well as (iii) to compare them with a commercial activated carbon. The structure of the preliminary assays was meant to narrow down the choice between adsorbents and find the best one and the conditions under which it performed better.

Therefore, all the carbons have been tested at different pHs, and then those that performed better have been tested in different S/L ratio conditions.

4.3.1 Adsorption assays at different initial pH values

Figure 6 presents the results obtained in the adsorption assays at different initial pH values for all the ACs.



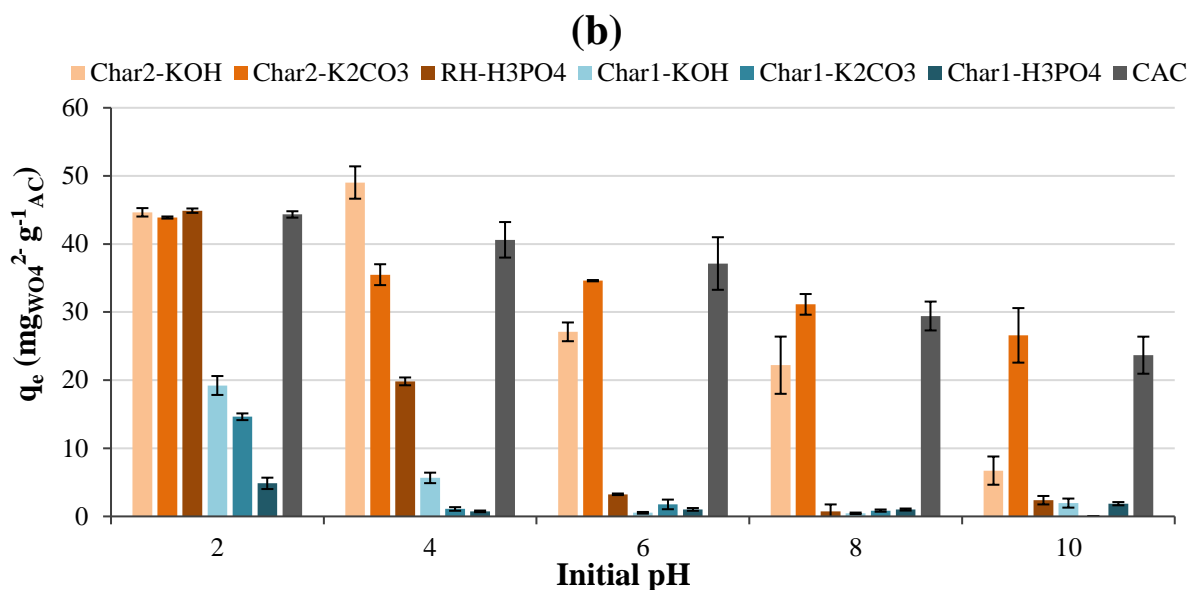


Figure 6. WO_4^{2-} removal efficiency (R) (a) and WO_4^{2-} uptake capacity (q_e) (b) of the ACs at different initial pH values. Experimental conditions: Initial WO_4^{2-} concentration = 50 mg L $^{-1}$; contact time = 24 h; S/L ratio = 1 g L $^{-1}$.

As in can be seen in Figure 6, the performances of the ACs were strongly dependent on the pH of the medium and on the textural and chemical properties of the ACs. The effect of the pH can be explained by considering the pH_{pzc} of the adsorbents. In fact, when the pH of a medium is below the pH_{pzc} of a solid matrix, its surface would be positively charged due to the release of hydroxyl groups and/or acquisition of protons (Babić et al., 1999; Kosmulski, 2009).

Considering that Tungstate is an oxyanion, a positively charged surface favored adsorption processes, especially because Tungsten is one of the elements that create Poly-oxometallates (POMs), which are massive ions formed by three or more oxyanions linked together by sharing oxygen atoms. POMs create wide and complex 3D structures and can have negative valences up to -10 (Patrick and Smith, 2000), as it can be seen from the speciation graphs of Tungsten in Figure 7. Therefore, strong electrostatic interaction can be formed between the negatively charged tungstate species and the positively charged carbon surface. The higher is the pH_{pzc} of a carbon (which is the case of carbons Char2-KOH, Char2-K₂CO₃, and CAC), the higher is the density of positive charges at carbons surface at a low pH of the medium. This is the reason for which the best adsorption results were obtained at pH values of 2 and 4.

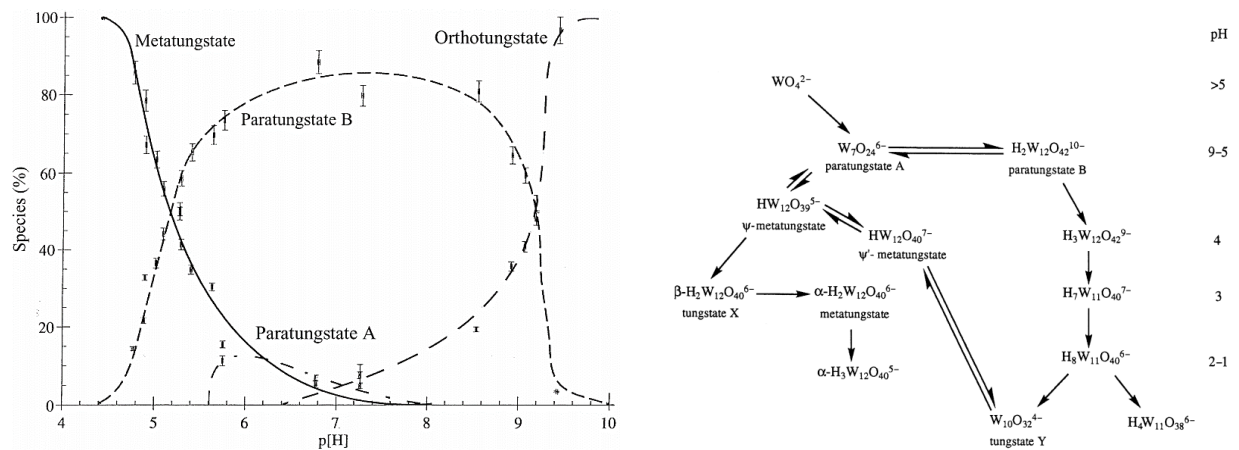


Figure 7. Tungsten speciation with pH (Patrick and Smith, 2000).

In addition to the chemical surface properties, textural properties also seemed to play a major role in the adsorption, since the carbons with higher surface areas and total pore volumes (Char2-KOH, Char2-K₂CO₃, RH-H₃PO₄) presented the highest WO₄²⁻ removal efficiencies and uptake capacities. Although CAC carbon presented slightly poorer textural properties compared to Char1-KOH sample, the commercial sample performed much better due to its quite high alkaline character.

The study on these assays induced to choose pH 2 as the operative pH for the following steps in the study of the synthetic solution. This consideration has been supported by the fact that in most of the Wolframite mines, the extraction of Tungsten is performed by an Hydrochloric leaching and a consequent separation in a strong acidic environment or alkaline environment depending on the unwanted chemical elements to remove (Trasorras et al., 2016).

4.3.2 Adsorption assays at different S/L ratios

After comparing the results obtained for the activated carbons produced from Char1 with the activated carbons obtained from Char2, at different pH values, it was possible to discarding some carbons, namely the Char1 series, and proceeding to study the effect of different S/L ratios fixing the pH at 2. Figure 8 presents the results obtained in the adsorption assays at different S/L ratios for the ACs from Char 2 series and CAC.

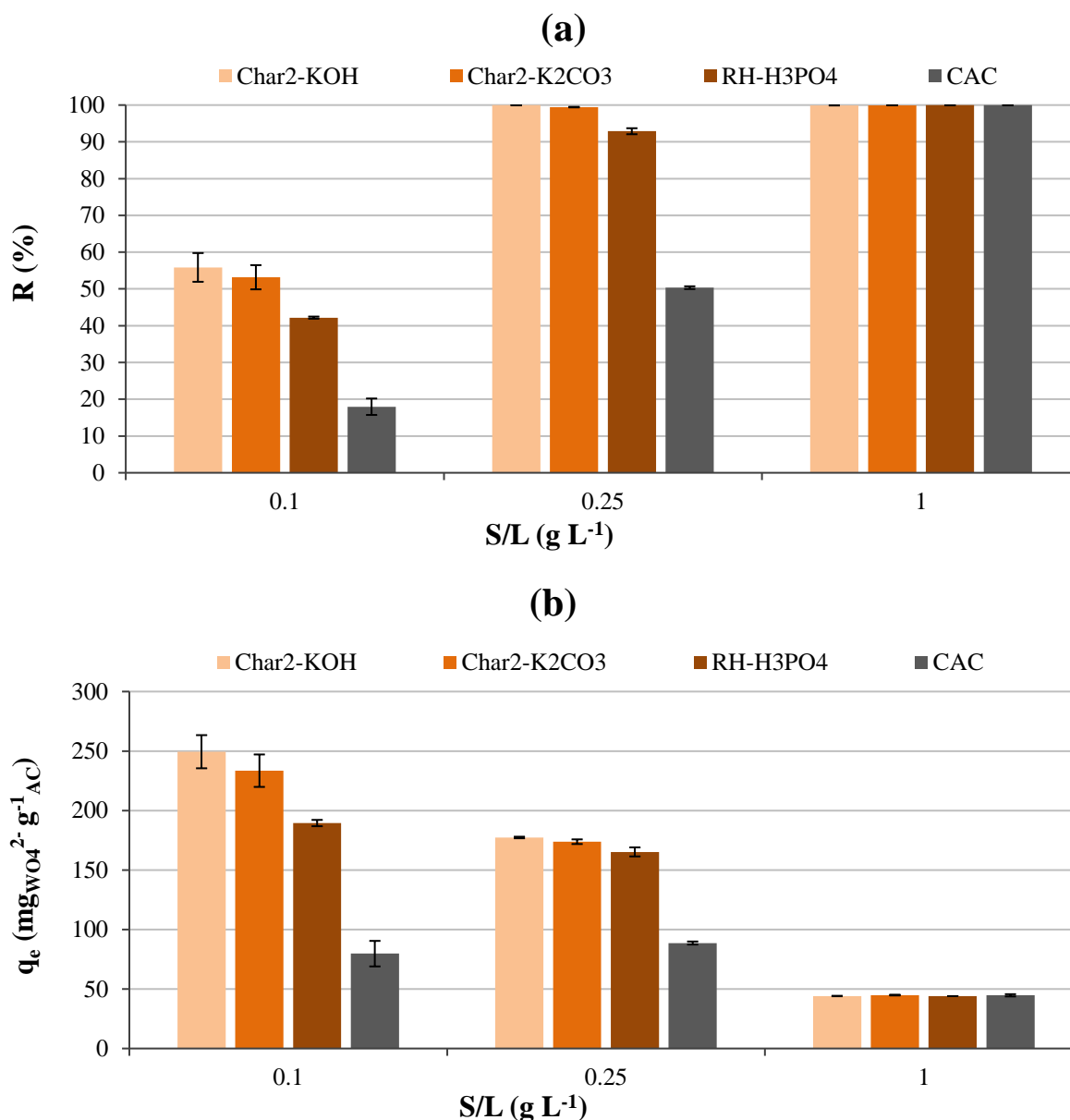


Figure 8. WO_4^{2-} removal efficiency (R) (a) and WO_4^{2-} uptake capacity (q_e) (b) of the ACs at different S/L ratios. Experimental conditions: Initial WO_4^{2-} concentration = 50 mg L^{-1} ; contact time = 24 h; Initial pH = 2.

As it can be seen in Figure 8, to change the S/L ratio affects the amount of adsorbate removed. None of the carbons achieved a complete removal at S/L 0.1 g L^{-1} because the porous material was saturated before removing all the adsorbate. This means that the porous volume of the adsorbent played a role in the process as well, and from the observation that the dominant species at pH 2 is the Metatungstate ion ($\alpha\text{-H}_2\text{W}_{12}\text{O}_{40}^{6-}$), it might be assumed that, considering the dimensions of this huge ion, the mesopore volume was the third variable (together with the surface area and the pH_{pzc} of the AC) affecting the adsorption mechanism. From the four carbons, CAC presented the lower

mesopore volume (Table 1) and this feature might have determined its worse performance when compared with the other carbons.

Char2-KOH was the adsorbent that presented the best performance in WO_4^{2-} adsorption in the two sets of preliminary assays. It seems that the combination of textural and chemical surface properties of this carbon established its high uptake capacity of tungstate. Therefore, this porous carbon was selected for the further assays (kinetic study and adsorption isotherm study).

4.3 KINETIC MODELLING

Char2-KOH and CAC were submitted to a kinetic study and the experimental kinetic data was then fitted to the pseudo-first order and pseudo-second order kinetic models. Table 5 presents the parameters obtained for the two kinetic models and their correlation coefficients R^2 , while Figure 9 presents the adsorption kinetic curves of WO_4^{2-} for both Char2-KOH and CAC samples.

Table 5. Kinetic parameters obtained with the applied kinetic models.

Kinetic	Kinetic parameter	Char2-KOH	CAC
Pseudo-First Order kinetic model	$k_f (\text{h}^{-1})$	12.7×10^{-2}	7.19×10^{-1}
	$q_e (\text{mg}_{\text{WO}_4^{2-}} \text{g}^{-1}_{\text{AC}})$	350	100
	R^2	0.939	0.885
Pseudo-Second Order kinetic model	$k_s (\text{g}_{\text{AC}} (\text{mg}_{\text{WO}_4^{2-}} \text{h})^{-1})$	6.52×10^{-2}	1.85×10^{-2}
	$q_e (\text{mg}_{\text{WO}_4^{2-}} \text{g}^{-1}_{\text{AC}})$	347	101
	R^2	0.9770	0.9255

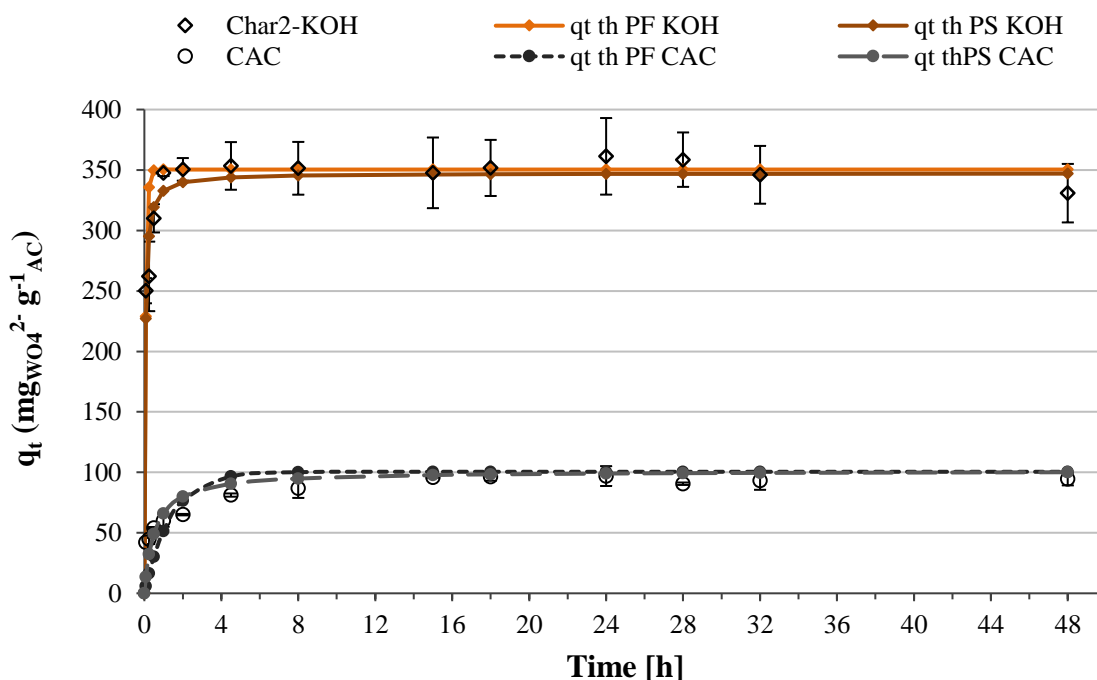


Figure 9. Kinetic data of WO_4^{2-} removal for Char2-KOH and CAC adjusted to kinetic models. Experimental conditions: Initial WO_4^{2-} concentration = 50 mg L^{-1} ; S/L ratio = 0.1 g L^{-1} ; Initial pH = 2. (qt th PF – theoretical uptake capacity calculated with pseudo-first order kinetic model; qt th PS – theoretical uptake capacity calculated with pseudo-second order kinetic model)

As it can be observed in Figure 9, the biomass-based carbon achieved significantly higher values of uptake capacity than CAC: $349.92 \pm 8.24 \text{ mg}_{\text{WO}_4^{2-}} \text{ g}^{-1}_{\text{AC}}$ against $94.56 \pm 2.37 \text{ mg}_{\text{WO}_4^{2-}} \text{ g}^{-1}_{\text{AC}}$ on average. Char2-KOH reached the equilibrium much faster than the commercial carbon, in fact it is possible to see a plateau in the adsorption curve already after 1 h while the CAC required around 15 h for stabilization. The Pseudo-Second order kinetic model gave a better fitting for both the ACs, with an R^2 of 0.98 for the Char2-KOH and 0.93 for the CAC. The higher kinetic constant, k_s , for Char2-KOH carbon is in accordance with the faster adsorption process promoted by this carbon.

4.4 ADSORPTION ISOTHERMS

The assays were performed with a contact time of 24 h even though the kinetic study showed that equilibrium is reached in a shorter time. This way it was ensured that full equilibrium conditions were achieved. Figure 10 presents the WO_4^{2-} removal efficiency and uptake capacity in a way to display how the initial concentration affects the performances of the ACs.

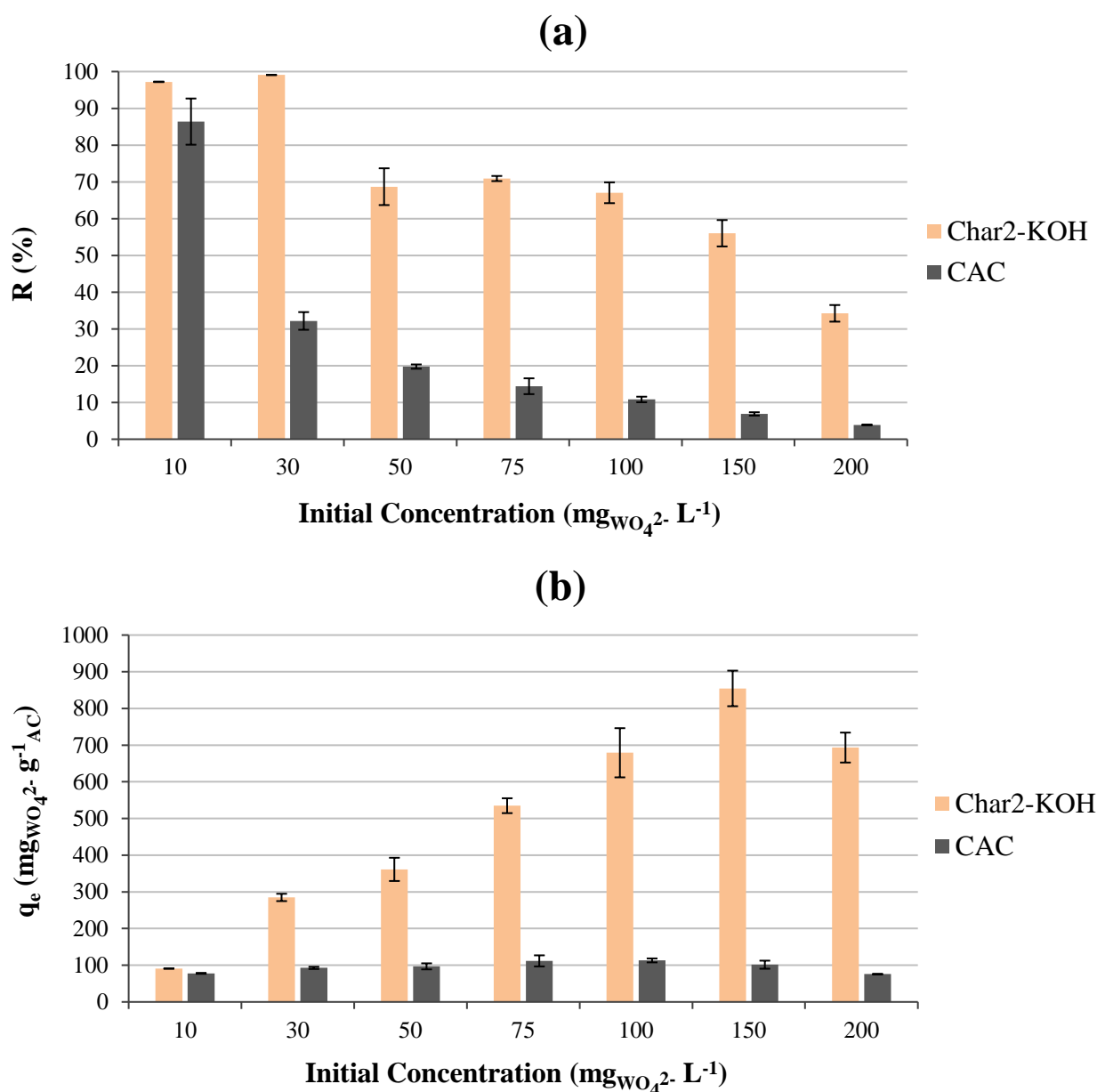


Figure 10. WO_4^{2-} removal efficiency (R) (a) and WO_4^{2-} uptake capacity (q_e) (b) of the ACs at different WO_4^{2-} initial concentrations. Experimental conditions: S/L ratio = 0.1 g L^{-1} ; contact time = 24 h; Initial pH = 2.

Figure 10a demonstrates how the Char2-KOH had a much higher efficiency in removing Tungstate from the medium in all the different concentrations. This means that the objective of identifying a biomass-based AC capable of performing better than a commercial one has been successfully achieved, at least when working with a synthetic solution. Figure 10b allowed to identify the optimal concentration for the adsorption. Since the uptake capacity, at a concentration of $200 \text{ mg}_{\text{WO}_4^{2-}} \cdot \text{L}^{-1}$, is lower than the one at $150 \text{ mg}_{\text{WO}_4^{2-}} \cdot \text{L}^{-1}$ for both carbons, this means that the maximum concentration should be kept around the latter value.

Comparing the results obtained in this work with similar adsorption studies from aqueous solutions, although they have been mostly performed by using mineral adsorbents (Table 6), it was possible to ascertain that the results obtained in the present work were outstandingly better than the data available in literature.

Table 6. Bibliographic comparison on the uptake capacities of different adsorbents for WO_4^{2-} from aqueous media.

Adsorbent	Activation/Treatment	Uptake capacity (mg g ⁻¹)	Reference
Pahokee peat	No	6.52 – 8.91	Sen Tuna and Braida, (2014)
Gibbsite	No	49.81	Iwai and Hashimoto, (2017)
Ferrihydride	No	0.607 – 37.0	Sun and Bostick, (2015)
Fly ash	No	4.72 – 7.62	Ogata et al., (2014)
	Hydrothermal treatment	21.72 – 74.12	
Montmorillonite clay	No	2.11 – 5.54	Gecol et al., (2006)
	Coated with chitosan	11.4 – 23.9	
Silica polyamine composites	Functionalized with phosphorus acid and Zr(IV) immobilization		Kailasam and Rosenberg, (2012)
	Polymer based adsorbents	No	
Char2-KOH (RH-based AC)	Yes		The present work
	Chemical Activation with KOH (impregnation ratio 1:4)	854	

To complete the study on the adsorption mechanisms of Tungstate, the experimental data of isotherms were fitted to different isotherm models. For the sake of clarity, Char2-KOH and CAC were presented in two different graphs (Figures 11 and 12) due to the eight-fold difference in their q_e values. Then to promote the comparison, Figure 13 presents only the best fitting model for both the ACs.

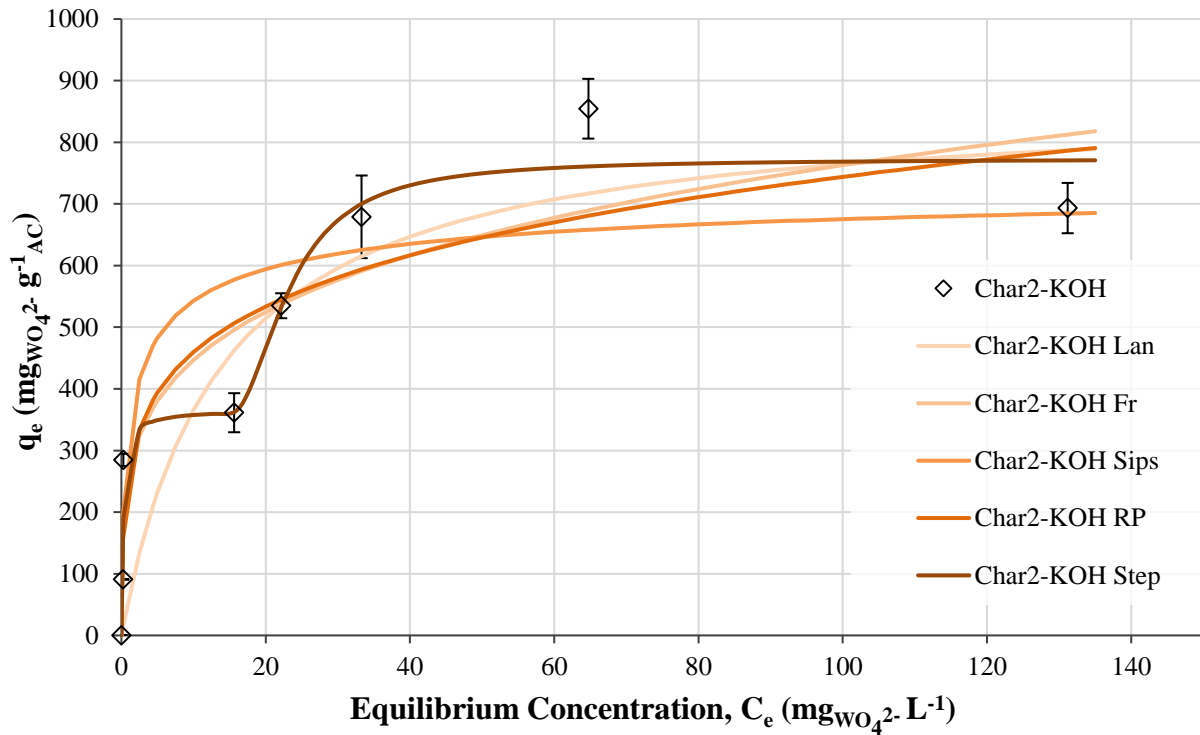


Figure 11. Adsorption isotherm models fitted to experimental data of the activated carbon Char2-KOH. (Lan – Langmuir model; Fr – Freundlich model; Sips – Sips model; RP – Redlich-Peterson model; Step – Step model).

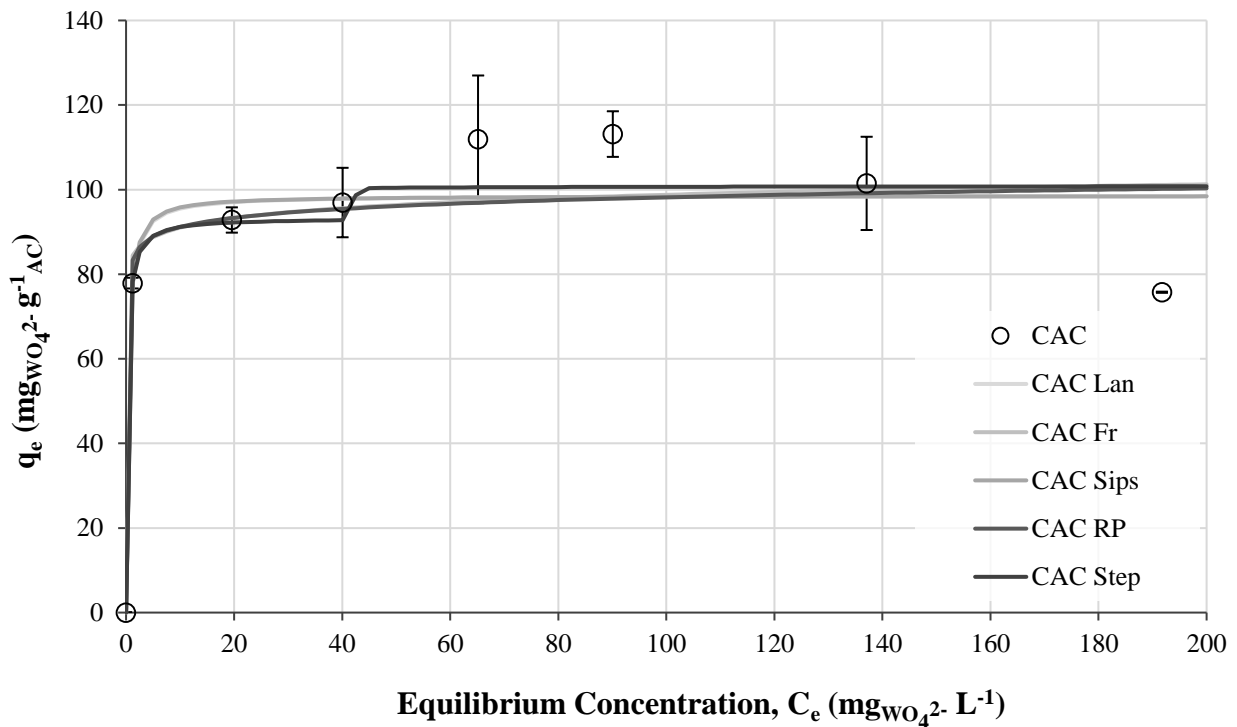


Figure 12. Adsorption isotherm models fitted to experimental data of the activated carbon CAC (Lan – Langmuir model; Fr – Freundlich model; Sips – Sips model; RP – Redlich-Peterson model; Step – Step model).

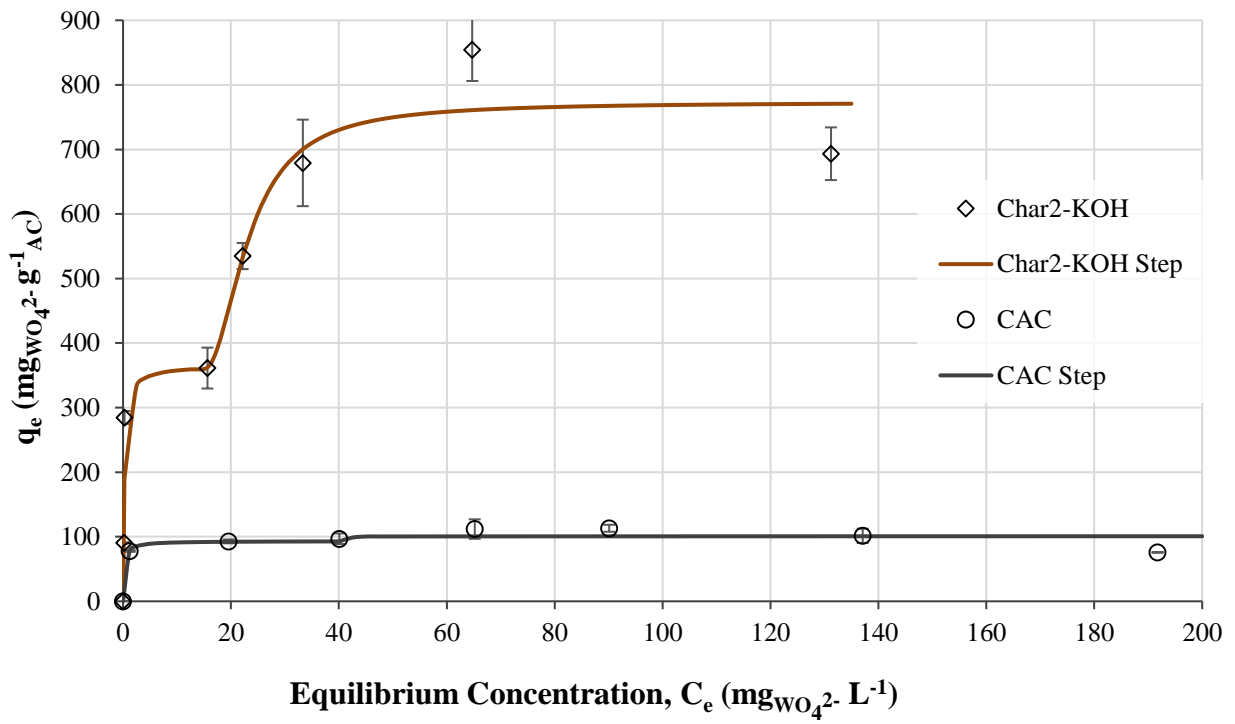


Figure 13. Step isotherm model applied on the experimental data of both ACs in order to compare the fitting results.

Table 7. Parameters of isotherm models for Char2-KOH and CAC

		CHAR2-KOH			CAC		
Models with 2 parameters							
Langmuir	$q_e = \frac{q_{max}bC_e}{1 + bC_e}$	q_{max}^a	870	$R^2 = 0.865$	$q_{max}^{(a)}$	98.7	$R^2 = 0.898$
		b^b	7.26×10^{-1}		$b^{(b)}$	3.04	
Freundlich	$q_e = k_F C_e^{1/n}$	k_F^c	261	$R^2 = 0.868$	$k_F^{(c)}$	83.8	$R^2 = 0.880$
h		n^d	4.31		$n^{(d)}$	28.1	
Models with 3 parameters							
Sip's	$q_e = \frac{q_{max}bC_e^{1/n}}{1 + bC_e^{1/n}}$	q_{max}^a	947	$R^2 = 0.831$	$q_{max}^{(a)}$	105	$R^2 = 0.890$
		b^b	6.00×10^{-1}		$b^{(b)}$	2.82	
		n^d	1.85		$n^{(d)}$	1.06	
Redlich-Peterson	$q_e = \frac{k_{RP}C_e}{1 + a_{RP}C_e^\beta}$	a_{RP}^e	6.99	$R^2 = 0.867$	$a_{RP}^{(e)}$	26.5	$R^2 = 0.883$
		k_{RP}^b	2071		$k_{RP}^{(b)}$	2262	
		β^d	7.99×10^{-1}		$\beta^{(f)}$	9.70×10^{-1}	
Model with 5 parameters							
Step Isotherm	$q_e = \sum_{i=1}^s \left\{ \frac{a_i k_i [(c - b_i) + abs(c - b_i)]^{n_i}}{2^{n_i} + k_i [(c - b_i) + abs(c - b_i)]^{n_i}} \right\}$	a_1^a	366	$R^2 = 0.949$	$a_1^{(e)}$	93.3	$R^2 = 0.901$
		a_2^a	407		$a_2^{(e)}$	7.58	
		k_1^b	4.07		$k_1^{(b)}$	4.24	
		K_2^b	1.44×10^{-2}		$K_2^{(b)}$	16.7	
		b_2^f	15.1		$b_2^{(g)}$	42.0	

a: $mg_{WO_4^{2-}} \cdot g_{AC}^{-1}$; b: $L (mg_{WO_4^{2-}})^{-1}$; c: $L g_{AC}^{-1}$; d: (Adimensional); e: $[L (mg_{WO_4^{2-}})^{-1}]^\beta$; f: $mg_{WO_4^{2-}} \cdot L^{-1}$.

The modeling confirmed that Tungsten follow a complex, two-step process, as it can be seen comparing the determination coefficients of the different models (Table 7).

It is noteworthy that even though the Sip and the Redlich-Peterson models introduce a third parameter, the former produced a worse fitting than the traditional models and the latter almost overlapped the Freundlich curve. Therefore, the poor fitting of the models assuming a single mechanism confirmed the hypothesis that the adsorption could be in fact a composition of different mechanisms.

This consideration is strongly supported by the chemistry of the metal element. Tungsten, as mentioned above, can form Poly-oxometallates and so its adsorption is likely composed by a first monolayer adsorption and a consequent solute-solute interaction, this way generating the second step in the experimental distribution.

Given the different properties of the CAC sample, the uptake capacity was significantly lower, but as it can be seen in Figure 13, when the two ACs are compared, the two-steps mechanism holds true even for the commercial adsorbent.

4.5 CHARACTERIZATION OF THE MINING WASTEWATER

The mining wastewater (before decantation) used in the present work presented the physical-chemical properties shown in Tables 8 and 9.

Table 8. pH, conductivity, density and content of solids on the mining wastewater.

Parameter	Value	Unit
pH	8.11 ± 0.03	Sørensen
Conductivity	2512 ± 16	$\mu\text{S cm}^{-1}$
Density	1015 ± 0	g L^{-1}
Total solids (TS)	250 ± 20	g L^{-1}
Fixed Solids (FS)	248 ± 20	g L^{-1}
Volatile Solids (VS)	2.0 ± 0.2	g L^{-1}
Suspended Solids (SS)	44.8 ± 0.9	g L^{-1}

Table 9. Mineral content of the mining wastewater, before and after decantation (Mean \pm Std. deviation; n = 2) and solubility assessment (%).

Element	Acidic Eluate (mg L ⁻¹)	Filtrate (mg L ⁻¹)	Solubility* (%)
Fe	23772 \pm 1484	(4.56 \pm 0.22) x10 ⁻²	1.92 x10 ⁻⁴
Al	9782 \pm 840	0.473 \pm 0.034	4.84 x10 ⁻³
Zn	5414 \pm 519	(4.10 \pm 0.39) x10 ⁻²	7.57 x10 ⁻⁴
K	4096 \pm 347	70.7 \pm 1.8	1.73
Mg	3472 \pm 317	69.4 \pm 0.5	2.00
Ca	2947 \pm 279	572 \pm 3	19.4
Cu	1080 \pm 99	< 3.80 x10 ⁻³	< 3.52 x10 ⁻⁴
Si	801 \pm 78	3.02 \pm 0.01	0.377
W	299 \pm 27	0.244 \pm 0.01	8.16 x10 ⁻²
V	18.4 \pm 1.8	< 2.00 x10 ⁻⁴	< 1.09 x10 ⁻³
Ni	15.2 \pm 1.0	< 4.00 x10 ⁻³	< 2.63 x10 ⁻²
Na	6.46 \pm 0.03	1.88 \pm 0.01	29.0

$$*Solubility = Filtrate/Acidic Eluate \times 100$$

The mining wastewater was slightly alkaline and with a high conductivity (Table 7) due to the high content of inorganic material, namely Fe but also Al, Zn, K, Mg and Ca (Table 8). However, a very low solubility was found for almost every element. Only Ca, K and Mg and Na presented a significant concentration in the filtrate (572, 7.7 and 69.4 mg L⁻¹, respectively) with a solubility of 19.4%, 2.00% and 1.73%. Also, Na presented a high solubility with a value of 29.0%, although its concentration in the filtrate was rather low (1.88 mg L⁻¹). This means that most elements are present in the solid fraction of the wastewater and presents a low mobility to the liquid fractions. W was quantified with a low concentration both in the acidic eluate and filtrate, since it is the main resource recovered in the extraction process. The closest equivalent to the filtrate that could be found in an industrial setting is the Tailing Dam Wastewater (TDW), which is the wastewater collected in the settling basins of Tungsten rocks mines. As shown in table 10, this type of medium can present very low concentration of every chemical species because, being stored in an open basin, it is exposed to ordinary rainfall and so presenting high dilution rates (Meng et al., 2018).

Table 10. Tailing Dam Water Characteristics (adapted from Meng et al., 2018; values in mg L⁻¹, except pH in Sørensen scale)

pH	Na	Mg	Al	Si	K	Ca	Fe	Mo
12.33	3.37	9.23 x10 ⁻²	0.312	45.4	18.1	96.1	2.15 x10 ⁻²	0.623

Concerning the ecotoxicity of the wastewater as it was delivered, the study showed no ecotoxicity for the bacterium *V. fischeri* as the EC₅₀–30 min was >99%. The Microtox® assay (ISO 11348-3) was repeated after the adsorption assays to investigate if the adsorption treatment affected its toxicity.

4.6 ADSORPTION ASSAYS IN MINING WASTEWATER

4.6.1 Batch assays

For the adsorption assays on the mining wastewater it was decided to spike the wastewater with W, as the concentration present in the filtrate was considerably below the ones tested in the synthetic solution. Given the results of the modelling procedure for the isotherms, the chosen concentration for the assays on the real effluent was fixed at 180 mg_{WO₄²⁻}L⁻¹. The procedure was the same as adopted for the batch assays in the synthetic solution. Figure 14 presents the removal efficiencies, *R*, and uptake capacities, *q_e*, of the selected ACs in the four different scenarios introduced in chapter 3.6.

The scenarios were:

- i. Wastewater with spiked Tungsten at the original pH;
- ii. Wastewater with spiked Tungsten at pH 2.

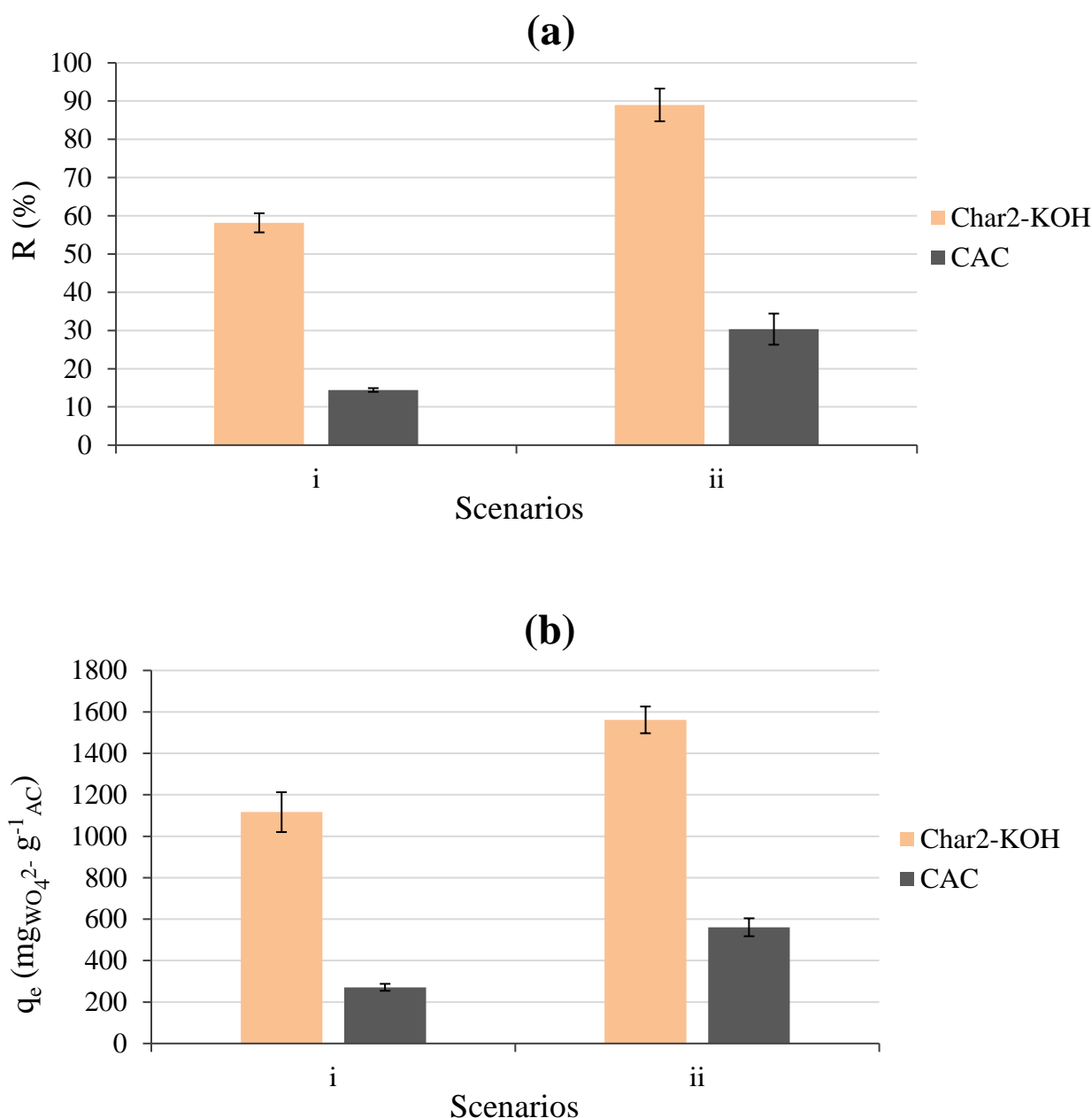


Figure 14. Removal efficiency (R) (a) and uptake capacity (q_e) (b) of the ACs Char2-KOH and CAC in the two different scenarios tested on the mining wastewater. Experimental conditions: S/L ratio = 0.1 g L^{-1} ; contact time = 24 h; Initial pH = 8.11 for the scenario *i* and pH = 2 for the scenario *ii*.

While the effluent was naturally quite poor in Tungstate, spiking its concentration showed that the optimal conditions determined with the synthetic solution are valid even for the mining wastewater. The presence of other ions determined a strong increase in the value of uptake capacity for the Char2-KOH in the industrial solution compared to the synthetic solution, i.e. $1561 \pm 64.57 \text{ mg}_{\text{WO}_4^{2-}} \cdot \text{g}^{-1}_{\text{AC}}$ in the former medium against $854 \pm 48.47 \text{ mg}_{\text{WO}_4^{2-}} \cdot \text{g}^{-1}_{\text{AC}}$ in the latter, and this can be explained by considering a salting-out effect. When there is a high concentration of dissolved salts in a medium (especially cations), their hydration due to the weak bonding between salt ions and

water ions, effectively reduces the volume of available solvent for the other species diffusion (Fang et al., 2015; Furter, 1977).

The main dissolved species in the solution, aside from W, were Ca, K, Mg. While Tungsten was the target of this study, the three cations were the main species involved in this phenomenon because Ca, Mg and K presented the highest hydration radius among single element ions: Mg^{2+} (0.395 nm) > Ca^{2+} (0.348 nm) > K^+ (0.315 nm) (Tanganov, 2014). This means that adding the reduced available medium to the strongly positive surface of the ACs due to the low pH system, forced a higher quantity of tungstate anions onto the carbon. This way, it makes the removal of Metatungstate from the mining wastewater (88.99 ± 4.28 %) even more efficient than the one accomplished at a comparable concentration in the synthetic solution (42.96 ± 2.79 %).

The higher removal efficiency obtained at pH 2, i.e. 88.99 ± 4.28 % against 58.16 ± 19.07 % at the original pH, confirmed the better option to work in acid conditions rather than at the original pH of the filtrate.

4.6.2. Ions interaction study

Comparing the concentrations of the main species in the filtrate before and after the adsorption batch allowed to assess how the other elements behaved in the process (ion-exchange mechanism, precipitation, complexation, etc.). The chosen chemicals were Al, Ca, Fe, K, Mg, Si and W, because they were present in the wastewater and/or in the ACs used in the adsorption assays. Figures 15 and 16 show the concentration variation of these elements at the original pH and at pH 2, respectively.

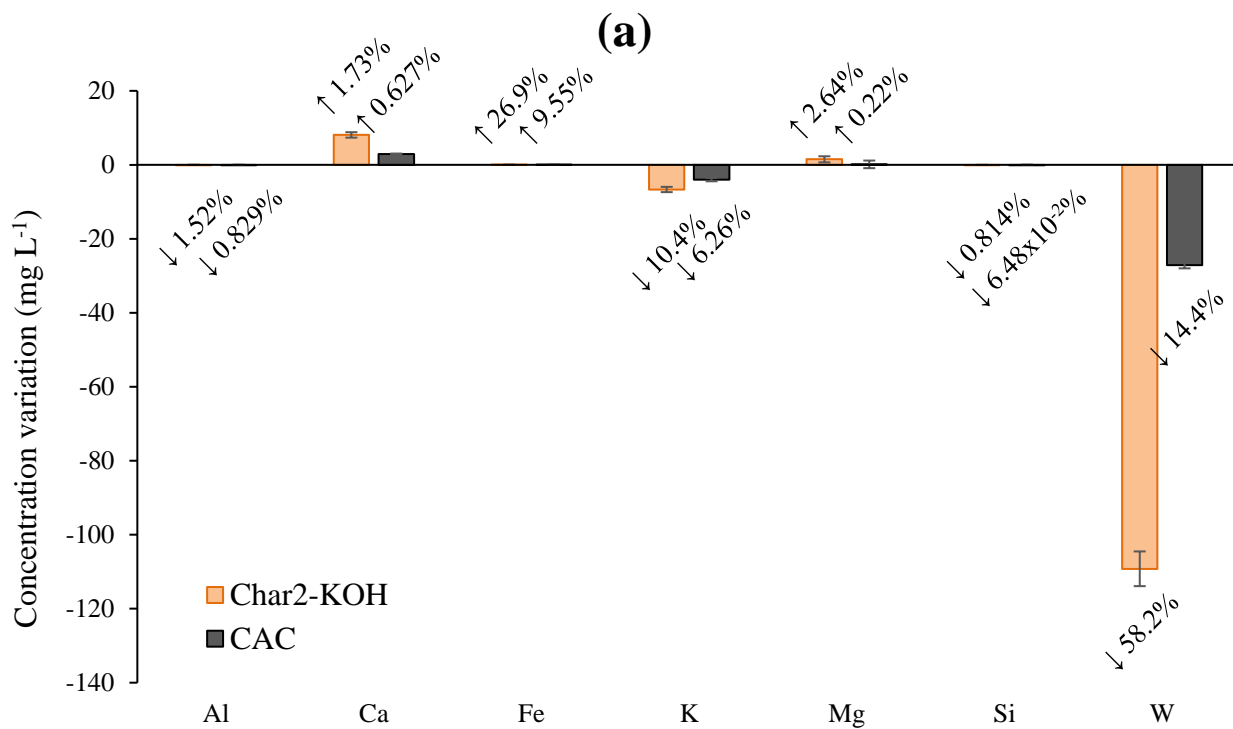


Figure 15. Concentration variation of the Char2-KOH and CAC in $\text{mgwo}_4^{2-} \text{L}^{-1}$ at pH 8.11 (original pH), scenario i.

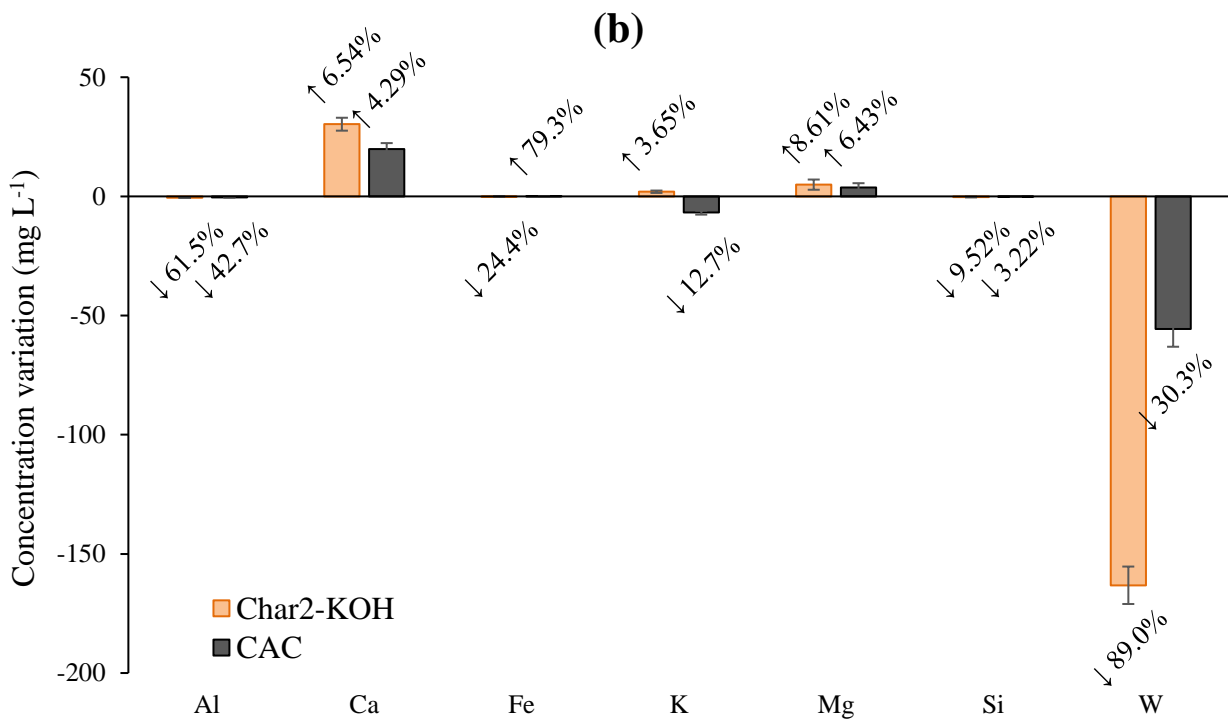


Figure 16. Concentration variation of the Char2-KOH and CAC in $\text{mgwo}_4^{2-} \text{L}^{-1}$ at (a) pH 8.11, scenario I, and at (b) pH 2, scenario ii.

As shown in Figures 15 and 16, the concentrations of the considered species didn't present any relevant variation, aside from slight changes of Ca and K concentrations, meaning that the elements were neither involved in competition mechanisms nor releasing/removal dynamics with the ACs. Ca was released from the carbons. In the samples with Char2-KOH calcium increased its concentration of 8.08 mg L⁻¹ at pH 8.11 and 30.29 mg L⁻¹ at pH 2 on an average concentration of 572 mg L⁻¹. Potassium on the other hand, had a reduction of 6.95 mg L⁻¹ at pH 8.11 and an increase of 1.95 mg L⁻¹ at pH 2 on an average concentration of 70.1 mg L⁻¹ for the Char2-KOH. These very low variations (as indicated by the variation percentages in the tags), confirm that the ions in the medium did determine an increase in the removal efficiency due to the salting-out effect. This result highlights the outstanding performance of the developed porous carbon from rice wastes in the removal/recovery of W, from a real effluent.

4.6.3. Ecotoxicological Study

Table 11 presents the results of the ecotoxicity study on the medium after the adsorption assays at the original pH and after correcting the pH.

Table 11. Ecotoxicity assessment of the mining wastewater before and after tungstate (WO₄²⁻) removal assays.

Scenario	EC ₅₀ -30 min, % v/v					
	Mining wastewater before the adsorption assays		Mining wastewater after the adsorption assays			
			Char2-KOH		CAC	
	Before pH correction	After pH correction	Before pH correction	After pH correction	Before pH correction	After pH correction
i	>99	n. a.	>99	n. a.	>99	n. a.
ii	1.61	>99	1.54	>99	1.48	>99

n.a. not applicable

It is observed that the wastewater at its original pH do not present ecotoxicity, neither before nor after the adsorption assays. As expected, at pH 2 the ecotoxicity was very significant because *V. fischeri* is very sensitive to pH variations. But in all situations, after pH correction no ecotoxicity was found.

5. CONCLUSIONS

The results achieved with the study were very significant in reinforcing the idea that adsorption can represent a highly valid strategy for recovering raw minerals from wastewaters, such as Tungsten, and that biomass-based porous carbon materials represent a much more sustainable alternative to adsorbents produced from mineral coal.

The optimized activated carbon, Char2-KOH, was in fact entirely based on pyrolyzed Rice Husk and achieved high performances relying on a quite standard activation procedure.

The study on the synthetic medium enabled to better understand how the speciation and protonation of the oxyanion are paramount in devising the best strategy to achieve a high removal of the compound, and which are the main characteristics that an adsorbent must have to successfully be employed in this treatment.

The highest removal efficiencies and uptake capacities were achieved with a pH of 2 and a S/L ratio of 0.1 g L^{-1} , and the main factors involved in the adsorption are the surface area of the carbons, volume of its mesopores and pH_{pzc} .

Even though there weren't enough data to build a solid model capable of explaining the relation between each factor and the results of the batch assays, it was possible to identify a direct correlation with the first two factors. The larger is the surface and volume of mesopores, the better is the removal.

Regarding the third factor (pH_{pzc}), it presented a direct correlation as well, but in this case its extent was also dependent on the pH of the medium. When working with an anion, to promote adsorption is necessary to have a positive charge on the carbon surface, therefore the pH of the solution must be much lower than the pH_{pzc} of the AC. In fact, Char1- H_3PO_4 , was the carbon with the lowest pH_{pzc} (equal to 2.38) and it achieved the lowest performance among all the ones tested.

Considering the factors involved in the process, the main removal mechanism seemed to be the electrostatic attraction of the W, as Metatungstate, or the formation of more complex species being attracted by the superficial charges on the adsorbent and trapped in its porous structure.

Testing the scenarios of the mining effluent with the spiked concentration was particularly useful in helping to establish the contribute of the "salting out effect" due to the high concentration of cations (especially iron in this case) in the real medium. These ions in fact, when in a very acid solution like the ones tested, aided in pushing the Metatungstate onto the carbon surface, promoting the adsorption and removal. This aided in achieving extremely high values of uptake capacity and much higher values compared to the synthetic medium, in which Tungstate was the only relevant species.

The study on the mining wastewater proved to be very important considering future feasibility and viability studies of the process in an industrial setting. Being able to achieve better performances than a commonly used commercial activated carbon was fundamental for evaluating the potential for upscaling to an actual industrial set up.

6. SCIENTIFIC OUTPUT

Currently being reviewed:

- Dias D., Don D., Jandosov J., Bernardo M., Fonseca I, Pinto F., Lapa N., 2019. Tungstate adsorption onto porous carbons obtained from rice wastes. WASTES: Solutions, treatments and Opportunities, 5th International Conference, 4-6 September, Caparica, Portugal.

REFERENCES

- Ahmad, M., Soo, S., Dou, X., Mohan, D., Sung, J., Yang, J.E., Sik, Y., 2012. Bioresource Technology Effects of pyrolysis temperature on soybean stover- and peanut shell-derived biochar properties and TCE adsorption in water. *Bioresour. Technol.* 118, 536–544. <https://doi.org/10.1016/j.biortech.2012.05.042>
- Ahmad, M., Upamali, A., Eun, J., Zhang, M., Bolan, N., Mohan, D., Vithanage, M., Soo, S., Sik, Y., 2014. Biochar as a sorbent for contaminant management in soil and water : A review. *Chemosphere* 99, 19–33. <https://doi.org/10.1016/j.chemosphere.2013.10.071>
- Ahmed, I.I., Nipattummakul, N., Gupta, A.K., 2011. Characteristics of syngas from co-gasification of polyethylene and woodchips. *Appl. Energy* 88, 165–174. <https://doi.org/10.1016/j.apenergy.2010.07.007>
- Akgün, O., Luukkanen, J., 2012. Extension of rice husk gasification technology for electricity generation in Cambodia. *Energy Procedia* 14, 1244–1249. <https://doi.org/10.1016/j.egypro.2011.12.1083>
- André, R.N., Pinto, F., Miranda, M., Carolino, C., Costa, P., 2014. Co-Gasification of Rice Production Wastes 39, 1633–1638. <https://doi.org/10.3303/CET1439273>
- Arena, U., Di Gregorio, F., 2014. Energy generation by air gasification of two industrial plastic wastes in a pilot scale fluidized bed reactor. *Energy* 68, 735–743. <https://doi.org/10.1016/j.energy.2014.01.084>
- Babić, B.M., Milonjić, S.K., Polovina, M.J., Kaludierović, B. V., 1999. Point of zero charge and intrinsic equilibrium constants of activated carbon cloth. *Carbon N. Y.* 37, 477–481. [https://doi.org/10.1016/S0008-6223\(98\)00216-4](https://doi.org/10.1016/S0008-6223(98)00216-4)
- Bansal, R.C., Goyal, M., 2005. *Activated Carbon Adsorption*. CRC Press, Boca Raton, FL 33487-2742.
- Bertini, F., Cacciamani, A., Canetti, M., 2017. Biofillers from rice husk for polymer composites, in: ISMAC-CNR (Ed.), *Book of Abstract. Eurofillers 2017*, Heraklion, p. 144.
- Binod, P., Sindhu, R., Singhanian, R.R., Vikram, S., Devi, L., Nagalakshmi, S., Kurien, N., Sukumaran, R.K., Pandey, A., 2010. Bioresource Technology Bioethanol production from rice straw : An overview. *Bioresour. Technol.* 101, 4767–4774. <https://doi.org/10.1016/j.biortech.2009.10.079>

- Burakov, A.E., Galunin, E. V., Burakova, I. V., Kucherova, A.E., Agarwal, S., Tkachev, A.G., Gupta, V.K., 2018. Adsorption of heavy metals on conventional and nanostructured materials for wastewater treatment purposes: A review. *Ecotoxicol. Environ. Saf.* 148, 702–712. <https://doi.org/10.1016/j.ecoenv.2017.11.034>
- Costa, P.A., Pinto, F.J., Ramos, A.M., Gulyurtlu, I.K., Cabrita, I.A., Bernardo, M.S., 2007. Kinetic Evaluation of the Pyrolysis of Polyethylene Waste 2489–2498.
- Czajczyńska, D., Nannou, T., Anguilano, L., Krzyżyńska, R., Ghazal, H., Spencer, N., Jouhara, H., 2017. Potentials of pyrolysis processes in the waste management sector. *Energy Procedia* 123, 387–394. <https://doi.org/10.1016/j.egypro.2017.07.275>
- Czinkota, I., Földényi, R., Lengyel, Z., Marton, A., 2002. Adsorption of propisochlor on soils and soil components equation for multi-step isotherms. *Chemosphere* 48, 725–731. [https://doi.org/10.1016/S0045-6535\(02\)00139-X](https://doi.org/10.1016/S0045-6535(02)00139-X)
- Dalglish, T., Williams, J.M.G., Golden, A.-M.J., Perkins, N., Barrett, L.F., Barnard, P.J., Au Yeung, C., Murphy, V., Elward, R., Tchanturia, K., Watkins, E., 2011. COM(2011)/0025 final -"Communication from the commission to the European Parliament, the Council, the European Economic and Social Committee and the Committee of the regions". Brussels.
- Delivand, M.K., Barz, M., Gheewala, S.H., 2011. Logistics cost analysis of rice straw for biomass power generation in Thailand. *Energy* 36, 1435–1441. <https://doi.org/10.1016/j.energy.2011.01.026>
- Deloitte Sustainability, British Geological Survey, Bureau de Recherches Géologiques et Minières, Research, N.O. for A.S., 2017. Study on the review of the list of Critical Raw Materials. Critical Raw Materials Factsheets. <https://doi.org/10.2873/876644>
- Dias, D., Lapa, N., Bernardo, M., 2018a. Programa PhD Doutoral em Program in Química Sustentável Sustainable Chemistry Recovery of metals with high commercial value through adsorption by chars from rice wastes (Rice2Metal).
- Dias, D., Lapa, N., Bernardo, M., Godinho, D., Fonseca, I., Miranda, M., Pinto, F., Lemos, F., 2017. Properties of chars from the gasification and pyrolysis of rice waste streams towards their valorisation as adsorbent materials. *Waste Manag.* 65, 186–194. <https://doi.org/10.1016/j.wasman.2017.04.011>
- Dias, D., Lapa, N., Bernardo, M., Ribeiro, W., Matos, I., Fonseca, I., Pinto, F., 2018b. Cr(III) removal from synthetic and industrial wastewaters by using co-gasification chars of rice waste streams. *Bioresour. Technol.* 266, 139–150. <https://doi.org/10.1016/j.biortech.2018.06.054>

- Directive (2008/98/EC), 2008. Directive 2008/98/EC of the European Parliament., Official Journal of the European Union. <https://doi.org/2008/98/EC.;32008L0098>
- EC - European Commission, 2014. Report on Critical raw Materials for the EU critical raw materials profiles. Brussels. [https://doi.org/Ref.Ares\(2015\)1819595-29/04/2015](https://doi.org/Ref.Ares(2015)1819595-29/04/2015)
- European Commission, 2011. Roadmap to a Resource Efficient Europe - COM(2011)571 -final, 2011. Brussels.
- Fang, J., Zhao, R., Wang, H., Li, C., Liu, J., 2015. Salting-out effect of ionic liquids on isobaric vapor-liquid equilibrium of acetonitrile-water system. *Chinese J. Chem. Eng.* 23, 1369–1373. <https://doi.org/10.1016/j.cjche.2015.04.011>
- Fang, X., Shen, Y., Zhao, J., Bao, X., Qu, Y., 2010. Status and prospect of lignocellulosic bioethanol production in China. *Bioresour. Technol.* 101, 4814–4819. <https://doi.org/10.1016/j.biortech.2009.11.050>
- Fao a, 2018. Rice Market Monitor.
- FAOb, n.d. FAOSTAT, “Food and Agriculture Organization of the United Nations”; <http://www.fao.org/faostat/en/#data/QC/> Last checked October 29th 2018 [WWW Document]. URL <http://www.fao.org/faostat/en/#data/QC/>
- Freundlich, H., 1907. Über die Adsorption in Lösungen." *Zeitschrift für Physikalische Chemie - Stöchiometrie und Verwandtschaftslehre. Zeitschrift für Phys. Chemie - Stöchiometrie und Verwandtschaftslehre* 57, 385–470.
- Fu, F., Wang, Q., 2011. Removal of heavy metal ions from wastewaters: A review. *J. Environ. Manage.* 92, 407–418. <https://doi.org/10.1016/j.jenvman.2010.11.011>
- Furter, W.F., 1977. Salt effect in distillation: A literature review II. *Can. J. Chem. Eng.* 55, 229–239. <https://doi.org/10.1002/cjce.5450550301>
- Gecol, H., Miakatsindila, P., Ergican, E., Hiibel, S.R., 2006. Biopolymer coated clay particles for the adsorption of tungsten from water. *Desalination* 197, 165–178. <https://doi.org/10.1016/j.desal.2006.01.016>
- GROW - Internal Market, D.D., 2017. COM(2017)/490 final.
- Hansen, V., Müller-Stöver, D., Ahrenfeldt, J., Holm, J.K., Birk Henriksen, U., Hauggaard-nielsen, H., 2014. Gasification biochar as a valuable by-product for carbon sequestration and soil amendment. *Biomass and Bioenergy* 72, 300–308. <https://doi.org/10.1016/j.biombioe.2014.10.013>
- Henrich, E., Bürkle, S., Meza-Renken, Z., Rumpel, S., 1999. Combustion and gasification kinetics of pyrolysis chars from waste and biomass. *J. Anal. Appl. Pyrolysis* 49, 221–241.

[https://doi.org/10.1016/S0165-2370\(98\)00119-3](https://doi.org/10.1016/S0165-2370(98)00119-3)

- Hirunpraditkoon, S., Tunthong, N., Ruangchai, A., Nuithitikul, K., 2011. Adsorption Capacities of Activated Carbons Prepared from Bamboo by KOH Activation. *Int. J. Chem. Mol. Eng.* 5, 477–481.
- Ho, Y.S., McKay, G., 1998. Sorption of dye from aqueous solution by peat. *Chem. Eng. J.* 70, 115–124. [https://doi.org/10.1016/S1385-8947\(98\)00076-X](https://doi.org/10.1016/S1385-8947(98)00076-X)
- Huang, Y., Chiueh, P., Shih, C., Lo, S., Sun, L., 2015. Microwave pyrolysis of rice straw to produce biochar as an adsorbent for CO₂ capture. *Energy* 1–8. <https://doi.org/10.1016/j.energy.2015.02.026>
- Iriarte-Velasco, U., Ayastuy, J.L., Zudaire, L., Sierra, I., 2014. An insight into the reactions occurring during the chemical activation of bone char. *Chem. Eng. J.* 251, 217–227. <https://doi.org/10.1016/j.cej.2014.04.048>
- Iwai, T., Hashimoto, Y., 2017. Adsorption of tungstate (WO₄) on birnessite, ferrihydrite, gibbsite, goethite and montmorillonite as affected by pH and competitive phosphate (PO₄) and molybdate (MoO₄) oxyanions. *Appl. Clay Sci.* 143, 372–377. <https://doi.org/10.1016/j.clay.2017.04.009>
- Iyagba, E.T., Mangibo, I.A., Mohammad, Y.S., 2009. The study of cow dung as co-substrate with rice husk in biogas production. *Sci. Res. Essays* 4, 861–866.
- Jabeen, M., Zeshan, Yousaf, S., Haider, M.R., Malik, R.N., 2015. High-solids anaerobic co-digestion of food waste and rice husk at different organic loading rates. *Int. Biodeterior. Biodegrad.* 102, 149–153. <https://doi.org/10.1016/j.ibiod.2015.03.023>
- Jandosov, J., Mansurov, Z.A., Bijsenbayev, M.A., Tulepov, M.I., Ismagilov, Z.R., Shikina, N. V., Ismagilov, I.Z., Andrievskaya, I.P., 2012. Synthesis of Microporous-Mesoporous Carbons from Rice Husk via H₃PO₄-Activation. *Adv. Mater. Res.* 602–604, 85–89. <https://doi.org/10.4028/www.scientific.net/amr.602-604.85>
- Jandosov, J.M., Mikhalovska, L.I., Howell, C.A., Chenchik, D.I., Kosher, B.K., Lyubchik, S.B., Silvestre-Albero, J., Ablaihanova, N.T., Srailova, G.T., Tuleukhanov, S.T., Mikhalovsky, S.V., 2017. Synthesis, Morphostructure, Surface Chemistry and Preclinical Studies of Nanoporous Rice Husk-Derived Biochars for Gastrointestinal Detoxification. *Eurasian Chem. J.* 19, 303. <https://doi.org/10.18321/ectj678>
- Kailasam, V., Rosenberg, E., 2012. Oxyanion removal and recovery using silica polyamine composites. *Hydrometallurgy* 129–130, 97–104. <https://doi.org/10.1016/j.hydromet.2012.08.010>

- Kosmulski, M., 2009. pH-dependent surface charging and points of zero charge. IV. Update and new approach. *J. Colloid Interface Sci.* 337, 439–448. <https://doi.org/10.1016/j.jcis.2009.04.072>
- Kwiatkowski, M., 2008. Application of fast multivariant identification technique of adsorption systems to analyze influence of production process conditions on obtained microporous structure parameters of carbonaceous adsorbents. *Microporous Mesoporous Mater.* 115, 314–331. <https://doi.org/10.1016/j.micromeso.2008.02.002>
- Lagergren, S.Y.D., 1898. About the theory of so-called adsorption of soluble substances. *Sven. Vetenskapsakad. Handlingar* 24, 1–39.
- Langmuir, I., 1918. Equação de Langmuir 345. <https://doi.org/10.1021/ja02242a004>
- Lehmann, J., Rillig, M.C., Thies, J., Masiello, C.A., Hockaday, W.C., Crowley, D., 2011. Soil Biology & Biochemistry Biochar effects on soil biota e A review. *Soil Biol. Biochem.* 43, 1812–1836. <https://doi.org/10.1016/j.soilbio.2011.04.022>
- Li, H., Dong, X., da Silva, E.B., de Oliveira, L.M., Chen, Y., Ma, L.Q., 2017. Mechanisms of metal sorption by biochars: Biochar characteristics and modifications. *Chemosphere* 178, 466–478. <https://doi.org/10.1016/j.chemosphere.2017.03.072>
- Lim, J.S., Abdul Manan, Z., Wan Alwi, S.R., Hashim, H., 2012. A review on utilisation of biomass from rice industry as a source of renewable energy. *Renew. Sustain. Energy Rev.* 16, 3084–3094. <https://doi.org/10.1016/j.rser.2012.02.051>
- Ma, L., Wang, T., Liu, Q., Zhang, X., Ma, W., Zhang, Q., 2012. A review of thermal – chemical conversion of lignocellulosic biomass in China. *Biotechnol. Adv.* 30, 859–873. <https://doi.org/10.1016/j.biotechadv.2012.01.016>
- Mastellone, M.L., Zaccariello, L., 2013. Gasification of polyethylene in a bubbling fluidized bed operated with the air staging. *Fuel* 106, 226–233. <https://doi.org/10.1016/j.fuel.2012.12.049>
- Meng, X., Wu, J., Kang, J., Gao, J., Liu, R., Gao, Y., Wang, R., Fan, R., Khoso, S.A., Sun, W., Hu, Y., 2018. Comparison of the reduction of chemical oxygen demand in wastewater from mineral processing using the coagulation–flocculation, adsorption and Fenton processes. *Miner. Eng.* 128, 275–283. <https://doi.org/10.1016/j.mineng.2018.09.009>
- Motta, I.L., Miranda, N.T., Maciel Filho, R., Wolf Maciel, M.R., 2018. Biomass gasification in fluidized beds: A review of biomass moisture content and operating pressure effects. *Renew. Sustain. Energy Rev.* 94, 998–1023. <https://doi.org/10.1016/j.rser.2018.06.042>
- Ogata, F., Iwata, Y., Kawasaki, N., 2014. Adsorption of Tungsten onto Zeolite Fly Ash Produced by Hydrothermally Treating Fly Ash in Alkaline Solution. *Chem. Pharm. Bull.* 62, 892–897.

<https://doi.org/10.1248/cpb.c14-00291>

- Patrick, V.A., Smith, B.J., 2000. Quantitative Determination of Sodium Metatungstate Speciation by ¹⁸³W N.M.R. Spectroscopy. *Aust. J. Chem.* 53, 965–970. <https://doi.org/10.1071/CH00140>
- Pérez-Marín, A.B., Zapata, V.M., Ortuño, J.F., Aguilar, M., Sáez, J., Lloréns, M., 2007. Removal of cadmium from aqueous solutions by adsorption onto orange waste. *J. Hazard. Mater.* 139, 122–131. <https://doi.org/10.1016/j.jhazmat.2006.06.008>
- Pinto, F., Costa, P., Gulyurtlu, I., Cabrita, I., 1999. Pyrolysis of plastic wastes. 1. Effect of plastic waste composition on product yield. *J. Anal. Appl. Pyrolysis* 51, 39–55. [https://doi.org/10.1016/S0165-2370\(99\)00007-8](https://doi.org/10.1016/S0165-2370(99)00007-8)
- Pinto, F., Miranda, M., Costa, P., 2015. Co-pyrolysis of Wastes Mixtures Obtained from Rice Production . Upgrading of Produced Liquids 43, 2053–2058. <https://doi.org/10.3303/CET1543343>
- Prasara-A, J., Gheewala, S.H., 2016. Sustainable utilization of rice husk ash from power plants: A review. *J. Clean. Prod.* 167, 1020–1028. <https://doi.org/10.1016/j.jclepro.2016.11.042>
- Redlich, O., Peterson, D.L., 1958. A Useful Adsorption Isotherm. *J. Physic Chem.* 63, 1024.
- Said, N., Bishara, T., García-maraver, A., Zamorano, M., 2013. Effect of water washing on the thermal behavior of rice straw. *Waste Manag.* 33, 2250–2256. <https://doi.org/10.1016/j.wasman.2013.07.019>
- Sangon, S., Hunt, A.J., Attard, T.M., Mengchang, P., Ngernyen, Y., Supanchaiyamat, N., 2017. Valorisation of waste rice straw for the production of highly effective carbon based adsorbents for dyes removal. *J. Clean. Prod.* 172, 1128–1139. <https://doi.org/10.1016/j.jclepro.2017.10.210>
- Satayeva, A.R., Howell, C.A., Korobeinyk, A. V., Jandosov, J., Inglezakis, V.J., Mansurov, Z.A., Mikhalovsky, S. V., 2018. Investigation of rice husk derived activated carbon for removal of nitrate contamination from water. *Sci. Total Environ.* 630, 1237–1245. <https://doi.org/10.1016/j.scitotenv.2018.02.329>
- Sathitruangsak, P., Madhiyanon, T., Soponronnarit, S., 2009. Rice husk co-firing with coal in a short-combustion-chamber fluidized-bed combustor (SFBC). *Fuel* 88, 1394–1402. <https://doi.org/10.1016/j.fuel.2008.11.008>
- Sen Tuna, G., Braida, W., 2014. Evaluation of the Adsorption of Mono- and Polytungstates onto Different Types of Clay Minerals and Pahokee Peat. *Soil Sediment Contam.* 23, 838–849. <https://doi.org/10.1080/15320383.2014.809049>

- Sharma, Y.C., Gupta, G.S., Prasad, G., Rupainwar, D.C., 1990. Use of wollastonite in the removal of Ni(II) from aqueous solutions. *Water. Air. Soil Pollut.* 49, 69–79. <https://doi.org/10.1007/BF00279511>
- Shen, Y., Zhao, P., Shao, Q., Ma, D., Takahashi, F., 2014. Applied Catalysis B : Environmental In-situ catalytic conversion of tar using rice husk char-supported nickel-iron catalysts for biomass pyrolysis / gasification. *"Applied Catal. B, Environ.* 152–153, 140–151. <https://doi.org/10.1016/j.apcatb.2014.01.032>
- Sips, R., 1948. On the structure of a catalyst surface. *J. Chem. Phys.* 16, 490–495. <https://doi.org/10.1063/1.1746922>
- Sizmur, T., Fresno, T., Akgül, G., Frost, H., Moreno-Jiménez, E., 2017. Biochar modification to enhance sorption of inorganics from water. *Bioresour. Technol.* 246, 34–47. <https://doi.org/10.1016/j.biortech.2017.07.082>
- Song, Q., Li, J., 2015. A review on human health consequences of metals exposure to e-waste in China. *Environ. Pollut.* 196, 450–461. <https://doi.org/10.1016/j.envpol.2014.11.004>
- Sun, J., Bostick, B.C., 2015. Effects of tungstate polymerization on tungsten(VI) adsorption on ferrihydrite. *Chem. Geol.* 417, 21–31. <https://doi.org/10.1016/j.chemgeo.2015.09.015>
- SWD(2014) 171 final, 2014. COM(2014)/297 final - Communication from the Commission to the European Parliament, the Council, the European Economic and Social Committee and the Committee of the regions. Brussels.
- SWD(2018) 36 final - Report on Critical Raw Materials and the Circular Economy, 2018. . Brussels. <https://doi.org/http://dx.doi.org/10.1016/j.dental.2013.08.006>
- Tan, X., Liu, Shao-bo, Liu, Y., Gu, Y., Zeng, G., Hu, X., Wang, X., Liu, Shao-heng, Jiang, L., 2016. Biochar as potential sustainable precursors for activated carbon production : multiple applications in environmental protection and energy storage. *Bioresour. Technol.* <https://doi.org/10.1016/j.biortech.2016.12.083>
- Tan, X., Liu, Y., Zeng, G., Wang, X., Hu, X., Gu, Y., 2015. Application of biochar for the removal of pollutants from aqueous solutions. *Chemosphere.* <https://doi.org/10.1016/j.chemosphere.2014.12.058>
- Tanganov, B.B., 2014. □ About the size of the hydrated salt ions - the components of sea water 64–67.
- Tolner, L., 2008. The determination of parameters of multi-step adsorption isotherm by sequential simplex optimization. *Appl. Ecol. Environ. Res.* 6, 109–117. <https://doi.org/10.15666/aeer/0604>

- Trasorras, J.R.L., Wolfe, T.A., Knabl, W., Venezia, C., Lemus, R., Lassner, E., Schubert, W.-D., Lüderitz, E., Wolf, H.-U., 2016. Tungsten, Tungsten Alloys, and Tungsten Compounds. *Ullmann's Encycl. Ind. Chem.* 1–53. https://doi.org/10.1002/14356007.a27_229.pub2
- Vitali, F., Parmigiani, S., Vaccari, M., Collivignarelli, C., 2013. Agricultural waste as household fuel : Techno-economic assessment of a new rice-husk cookstove for developing countries. *Waste Manag.* 33, 2762–2770. <https://doi.org/10.1016/j.wasman.2013.08.026>
- Wang, J., Kaskel, S., 2012. KOH activation of carbon-based materials for energy storage. *J. Mater. Chem.* 22, 23710–23725. <https://doi.org/10.1039/c2jm34066f>
- Yahya, M.A., Al-Qodah, Z., Ngah, C.W.Z., 2015. Agricultural bio-waste materials as potential sustainable precursors used for activated carbon production: A review. *Renew. Sustain. Energy Rev.* 46, 218–235. <https://doi.org/10.1016/j.rser.2015.02.051>
- Zhou, C., Liu, Z., Huang, Z.L., Dong, M., Yu, X.L., Ning, P., 2015. A new strategy for co-composting dairy manure with rice straw: Addition of different inocula at three stages of composting. *Waste Manag.* 40, 38–43. <https://doi.org/10.1016/j.wasman.2015.03.016>